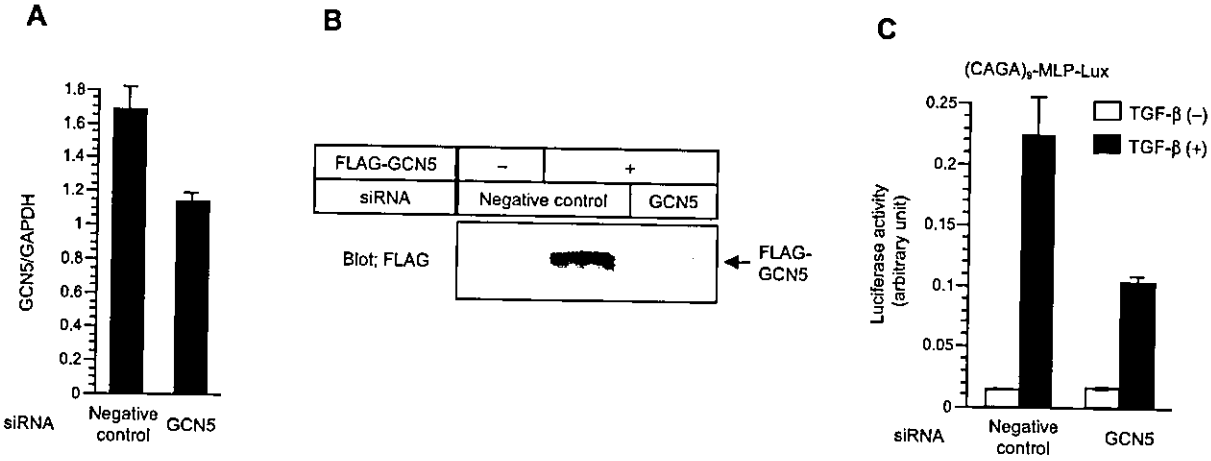

Figure 5 Effect of decreased expression level of GCN5 on TGF-β signalling. Effect of RNAi specific for GCN5 on endogenous expression level of (A) mRNA for GCN5 or (B) protein for GCN5. 293T cells were transfected with RNAi oligonucleotides corresponding to GCN5 (A) without or (B) with an expression plasmid for FLAG-GCN5. Twenty-four hours after transfection, GCN5 mRNA or protein was analysed (A) by real-time PCR or (B) by immunoblotting using anti-FLAG M2 antibody, respectively. (C) repression of TGF-β-dependent transactivation in the presence of RNAi for GCN5. 293T cells were transfected with RNA oligonucleotides of the indicated RNAi, and $(CAGA)_9$-MLP-lux. Cells were treated with 40 pM TGF-β3 for 24 h and luciferase activity was determined.

interacts with Smad3 through multiple regions (Nishihara *et al.* 1998). GCN5 and PCAF are structurally similar, especially in their C-terminal regions, which contain the HAT and bromo domains. The similarity of the C-terminal region is 83.1%, whereas that of the N-terminal region is only 63.3%. This data adds support to our suggestion that the N-terminal region of GCN5, but not of PCAF, affects the interaction with R-Smads. It will be interesting to determine the role of N-terminal region of GCN5 and PCAF in Smad signalling pathway in the future.

Multiple transcriptional coactivators appear to be incorporated into Smad transcriptional complexes. Among these coactivators, GCN5 and PCAF are similar in their structures, acetyltransferase activity and substrate specificity. Both of the coactivators are expressed ubiquitously in adult mammalian tissues, but their expression profiles are distinct, although likely to be complementary, in many tissues (Xu *et al.* 1998). In contrast to PCAF, however, GCN5 is able to facilitate both TGF-β and BMP signalling, suggesting the differences in physiological functions between GCN5 and PCAF *in vivo*. p300 has also been shown to interact with Smads and facilitate transcription induced by TGF-β (Feng *et al.* 1998; Janknecht *et al.* 1998; Nishihara *et al.* 1998; Shen *et al.* 1998). However, it is currently not known whether loss of p300/CBP results in perturbations of TGF-β signalling. In the present study, however, we have shown that loss of expression of GCN5 resulted in significant decrease in the transcription induced by TGF-β. Thus, our findings strongly suggest that GCN5 is an essential component in transcriptional regulation induced by TGF-β in certain cells. In the future, it will be interesting to determine how the balance of the multiple transcriptional coactivators regulates the response of cells to TGF-β superfamily proteins.

Experimental procedures

Cell culture

COS7 cells, R mutant Mv1Lu cells (R4-2 cells), 293T cells, and HaCaT human keratinocyte cells were cultured in Dulbecco's modified Eagle's medium (DMEM) supplemented with 10% foetal bovine serum (FBS) and antibiotics. C2C12 cells were cultured in DMEM containing 20% FBS and antibiotics. To establish stable transfectants, HaCaT cells were transfected with pcDNA3-FLAG-GCN5 by Effectene transfection reagent (Qiagen) and cultured in the presence of 1 mg/mL of G418 sulphate (Gibco) for transfectant selection. After selection, FLAG-GCN5 transfectants were maintained in DMEM containing 10% FBS and 0.5 mg/mL of G418 sulphate. Nuclear extract from MCF-7 cell was prepared as previously described (Kitagawa *et al.* 2003).

Plasmid constructions

The original constructions of constitutively active forms of TGF-β type I and BMP type IB receptors (TβR-I(TD) and BMP-IB(QD), respectively), and Smad1, Smad2, Smad3, Smad4, Smad5, Smad8, and the Smad3 deletion mutants, were previously

described (Nishihara *et al.* 1998; Kawabata *et al.* 1998). The expression vector for full-length GCN5 was previously described (Yanagisawa *et al.* 2002). Deletion mutants of GCN5 were generated by a polymerase chain reaction (PCR)-based approach from a full-length GCN5 cDNA. The expression vector for PCAF was kindly provided by Dr Itoh (Itoh *et al.* 2000).

DNAP

MCF-7 cell nuclear extract was precleared with 30 pmol of biotinylated mutated 3xCAGA and 50 μg of Dynabeads M-280 streptavidin (Dynal) at 4 °C for 30 min. The supernatant was collected and incubated with 30 pmol of biotinylated wild-type or mutated 3xCAGA and 12 μg of poly(dI-dC) at 4 °C overnight. DNA-bound proteins were precipitated with 100 μL of Dynabeads for 30 min at 4 °C, washed, separated with SDS-PAGE, and the resulting SDS-PAGE gel silver-stained. The sequences of wild-type 3xCAGA are: 5′-TCGAGAGCCAGACAAGGAGCCAGACAAGGAGCCAGACACTCGAG-3′ (sense strand) and 5′-CTCGAGTGTCTGGCTCCTTGTCTGGCTCCTTGTCTGGCTCTCGA-3′ (anti-sense strand) (Nishihara *et al.* 1999). The sequences of mutated 3xCAGA are: 5′-TCGAGAGCTACATAAAAAGCTACATATTTAGCTACATACTCGA-3′ (sense strand) and 5′-AGCTCTCGATGTATTTTTCGATGTATAAATCGATGTATGAGCT-3′ (anti-sense strand).

Protein identification

Selected protein-containing bands were excised from silver-stained SDS-PAGE gels, digested in-gel with trypsin, and subjected Autoflex (Bruker) as essentially described (Kanamoto *et al.* 2002). The searches for protein identification using the obtained peptide mass spectra were performed in the NCBInr sequence database using ProFound <http://prowl.rockfeller.edu/cgi-bin/proFound>.

Transfection, immunoprecipitation, and immunoblotting

COS7 cells were transiently transfected using FuGENE6 transfection reagent (Roche Applied Science), and were then lysed with Nonidet P-40 lysis buffer (20 mM Tris-HCl, pH 7.5, 150 mM NaCl, 1% Nonidet P-40). Immunoprecipitation and immunoblotting were performed as previously described (Ebisawa *et al.* 2001).

ChIP and real-time PCR

FLAG-GCN5 transfected cells (1×10^6 cells) were cross-linked by addition of 1% formaldehyde for 10 min and glycine added (0.125 M final) for 5 min to stop the cross-linking reaction. Soluble chromatin was prepared using ChIP assay kit (Upstate) according to the manufacturer's recommendations, and immunoprecipitated with either anti-FLAG M2 antibody (Sigma) or anti-Smad2/3 antiserum (Nakao *et al.* 1997). Following washes and elution, precipitates were heated overnight at 65 °C to reverse cross-linking. DNA fragments were purified using the QIAquick PCR purification kit (Qiagen). Quantitative real-time PCR analysis was performed with an ABI PRISM 7000 sequence detection system (Applied Biosystems), using a SYBR Green PCR master mix (Applied Biosystems). Optimal PCR conditions were found to be 50 °C for 2 min and 95 °C for 10 min, followed by 45 cycles of PCR consisting of 15 s at 95 °C, and 1 min at 60 °C. Specific primer pairs were designed to amplify a target sequence within the human PAI-1 promoter (5′-GCAGGACATCCGGGAGAGA-3′ and 5′-CCAATAGCCTTGGCCTGAGA-3′) and the human GAPDH gene, an external standard (5′-GCACCACCAACTGCTTAGCA-3′ and 5′-CACGATACCAAAGTTGTCATGGAT-3′).

Luciferase assay

R4-2 cells or 293T cells were transiently transfected with an appropriate combination of Gal4-M1-Lux (Itoh *et al.* 2000) $(CAGA)_9$-MLP-Lux (Dennler *et al.* 1998), or Id-1-MLP-Lux promoter-reporter constructs (Korchynskyi & ten Dijke 2002), expression plasmids, and pcDNA3. Total amounts of transfected DNAs were the same in each experiment. Luciferase activity was measured by a dual-luciferase reporter assay system (Promega), and values were normalized by Renilla luciferase activity.

RNAi

RNAi was performed as previously described (Kisielow *et al.* 2002). Briefly, RNAi oligonucleotides were introduced into 293T cells using the Lipofectamine 2000 reagent (Invitrogen), with 100 pmol of oligonucleotides and 5 μL of transfection reagent/well in a 12-well tissue culture plate, according to the manufacturer's introductions. RNA oligonucleotides corresponding to GCN5 (forward: 5′-AAGGAAGAGGACACAGGGAAGAGGACACAGACACC-3′; reverse: 5′-AAGGAAGAGGACACAGACACCGGGUCUGUGUCCUCUUCC-3′) were synthesized (Dharmacon). Blast analysis was used to confirm that negative control RNAi oligonucleotides were not complementary to any mammalian mRNA sequence. 293T cells were transfected with RNAi oligonucleotides and $(CAGA)_9$-MLP-Lux promoter-reporter or FLAG-GCN5 constructs using Lipofectamine 2000 reagent.

Reverse transcription and real-time PCR

Total cellular RNA was extracted using Trizol reagent (Invitrogen), and cDNA was synthesized using Superscript III first-strand synthesis system (Invitrogen). Quantitative real-time PCR analysis was performed as described above. The primer sequences used were as follows; human GCN5, forward: 5′-CTGAAGACCATGACTGAGCGG-3′, human GCN5, reverse: 5′-TCGGCCACAAAGAGCTTCC-3′; and human GAPDH, forward: 5′-GAAGGTGAAGGTCGGAGTC-3′, human GAPDH, reverse: 5′-GAAGATGGTGATGGGATTTC-3′.

Acknowledgements

We are grateful to Yuri Inada and Aki Hanyu for technical help. This study was supported by Grants-in-Aid for Scientific Research of the

Ministry of Education, Culture, Sports, Science, and Technology of Japan. This work was also supported by Nippon Boehringer Ingerheim and Viral Hepatitis Research Foundation of Japan.

References

Akiyoshi, S., Inoue, H., Hanai, J., *et al.* (1999) c-Ski acts as a transcriptional co-repressor in transforming growth factor-β signaling through interaction with Smads. *J. Biol. Chem.* **274**, 35269–35277.

Bannister, A.J. & Kouzarides, T. (1996) The CBP co-activator is a histone acetyltransferase. *Nature* **384**, 641–643.

Candau, R., Moore, P.A., Wang, L., *et al.* (1996) Identification of human proteins functionally conserved with the yeast putative adaptors ADA2 and GCN5. *Mol. Cell. Biol.* **16**, 593–602.

Dennler, S., Itoh, S., Vivien, D., ten Dijke, P., Huet, S. & Gauthier, J.-M. (1998) Direct binding of Smad3 and Smad4 to critical TGF β-inducible elements in the promoter of human plasminogen activator inhibitor-type 1 gene. *EMBO J.* **17**, 3091–3100.

Ebisawa, T., Fukuchi, M., Murakami, G., *et al.* (2001) Smurf1 interacts with transforming growth factor-β type I receptor through Smad7 and induces receptor degradation. *J. Biol. Chem.* **276**, 12477–12480.

Feng, X.H., Zhang, Y., Wu, R.-Y. & Derynck, R. (1998) The tumor suppressor Smad4/DPC4 and transcriptional adaptor CBP/p300 are coactivators for Smad3 in TGF-β-induced transcriptional activation. *Genes Dev.* **12**, 2153–2163.

Heldin, C.-H., Miyazono, K. & ten Dijke, P. (1997) TGF-β signalling from cell membrane to nucleus through SMAD proteins. *Nature* **390**, 465–471.

Itoh, S., Ericsson, J., Nishikawa, J., Heldin, C.-H. & ten Dijke, P. (2000) The transcriptional co-activator P/CAF potentiates TGF-β/Smad signaling. *Nucl. Acids Res.* **28**, 4291–4298.

Janknecht, R., Wells, J.N. & Hunter, T. (1998) TGF-β-stimulated cooperation of Smad proteins with the coactivators CBP/p300. *Genes Dev.* **12**, 2114–2119.

Kanamoto, T., Hellman, U., Heldin, C.-H. & Souchelnytskyi, S. (2002) Functional proteomics of transforming growth factor-β1-stimulated Mv1Lu epithelial cells: Rad51 as a target of TGFβ1-dependent regulation of DNA repair. *EMBO J.* **21**, 1219–1230.

Kato, Y., Habas, R., Katsuyama, Y., Naar, A.M. & He, X. (2002) A component of the ARC/Mediator complex required for TGF β/Nodal signalling. *Nature* **418**, 641–646.

Kawabata, M., Inoue, H., Hanyu, A., Imamura, T. & Miyazono, K. (1998) Smad proteins exist as monomers in vivo and undergo homo- and hetero-oligomerization upon activation by serine/threonine kinase receptors. *EMBO J.* **17**, 4056–4065.

Kisielow, M., Kleiner, S., Nagasawa, M., Faisal, A. & Nagamine, Y. (2002) Isoform-specific knockdown and expression of adaptor protein ShcA using small interfering RNA. *Biochem. J.* **363**, 1–5.

Kitagawa, H., Fujiki, R., Yoshimura, K., *et al.* (2003) The chromatin-remodeling complex WINAC targets a nuclear receptor to promoters and is impaired in Williams syndrome. *Cell* **113**, 905–917.

Korchynskyi, O. & ten Dijke, P. (2002) Identification and functional characterization of distinct critically important bone morphogenetic protein-specific response elements in the Id1 promoter. *J. Biol. Chem.* **277**, 4883–4891.

Liu, F., Hata, A., Baker, J.C., *et al.* (1996) A human Mad protein acting as a BMP-regulated transcriptional activator. *Nature* **381**, 620–623.

Liu, F., Pouponnot, C. & Massagué, J. (1997) Dual role of the Smad4/DPC4 tumor suppressor in TGFβ-inducible transcriptional complexes. *Genes Dev.* **11**, 3157–3167.

Nakao, A., Roijer, E., Imamura, T., *et al.* (1997) Identification of Smad2, a human Mad-related protein in the transforming growth factor β signaling pathway. *J. Biol. Chem.* **272**, 2896–2900.

Nishihara, A., Hanai, J., Imamura, T., Miyazono, K. & Kawabata, M. (1999) E1A inhibits transforming growth factor-β signaling through binding to Smad proteins. *J. Biol. Chem.* **274**, 28716–28723.

Nishihara, A., Hanai, J., Okamoto, N., *et al.* (1998) Role of p300, a transcriptional coactivator, in signalling of TGF-β. *Genes Cells* **3**, 613–623.

Roberts, A.B. & Sporn, M.B. (1990) The transforming growth factor-βs. In: *Peptide Growth Factors and Their Receptors, Part I* (eds M.B. Sporn & A.B. Roberts), pp. 419–472, Heidelberg: Springer-Verlag.

Shen, X., Hu, P.P., Liberati, N.T., Datto, M.B., Frederick, J.P. & Wang, X.-F. (1998) TGF-β-induced phosphorylation of Smad3 regulates its interaction with coactivator p300/CREB-binding protein. *Mol. Biol. Cell* **9**, 3309–3319.

Shi, Y. & Massagué, J. (2003) Mechanisms of TGF-β signaling from cell membrane to the nucleus. *Cell* **113**, 685–700.

Smith, E.R., Belote, J.M., Schiltz, R.L., *et al.* (1998) Cloning of Drosophila GCN5: conserved features among metazoan GCN5 family members. *Nucl. Acids Res.* **26**, 2948–2954.

Stroschein, S.L., Wang, W., Zhou, S., Zhou, Q. & Luo, K. (1999) Negative feedback regulation of TGF-β signaling by the SnoN oncoprotein. *Science* **286**, 771–774.

Wang, L., Mizzen, C., Ying, C., *et al.* (1997) Histone acetyltransferase activity is conserved between yeast and human GCN5 and is required for complementation of growth and transcriptional activation. *Mol. Cell. Biol.* **17**, 519–527.

Wotton, D., Lo, R.S., Lee, S. & Massagué, J. (1999) A Smad transcriptional corepressor. *Cell* **97**, 29–39.

Xu, W., Edmondson, D.G. & Roth, S.Y. (1998) Mammalian GCN5 and P/CAF acetyltransferases have homologous amino-terminal domains important for recognition of nucleosomal substrates. *Mol. Cell. Biol.* **18**, 5659–5669.

Yagi, K., Goto, D., Hamamoto, T., Takenoshita, S., Kato, M. & Miyazono, K. (1999) Alternatively spliced variant of Smad2 lacking exon 3. Comparison with wild-type Smad2 and Smad3. *J. Biol. Chem.* **274**, 703–709.

Yamauchi, T., Yamauchi, J., Kuwata, T., *et al.* (2000) Distinct but overlapping roles of histone acetylase PCAF and of the closely related PCAF-B/GCN5 in mouse embryogenesis. *Proc. Natl. Acad. Sci. USA* **97**, 11303–11306.

Yanagisawa, J., Kitagawa, H., Yanagida, M., *et al.* (2002) Nuclear receptor function requires a TFTC-type histone acetyl transferase complex. *Mol. Cell* **9**, 553–562.

Received: 30 October 2003
Accepted: 19 November 2003

The EMBO Journal (2004) 23, 4813–4823 | © 2004 European Molecular Biology Organization | All Rights Reserved 0261-4189/04
www.embojournal.org

THE EMBO JOURNAL

Ligand-dependent switching of ubiquitin–proteasome pathways for estrogen receptor

Yukiyo Tateishi[1,6], Yoh-ichi Kawabe[1,6], Tomoki Chiba[2], Shigeo Murata[2], Ken Ichikawa[1], Akiko Murayama[1], Keiji Tanaka[2], Tadashi Baba[1], Shigeaki Kato[3,4] and Junn Yanagisawa[1,5,*]

[1]Graduate School of Life and Environmental Sciences, University of Tsukuba, Tsukuba Science City, Ibaraki, Japan, [2]The Tokyo Metropolitan Institute of Medical Science, Bunkyo-ku, Tokyo, Japan, [3]Institute of Molecular and Cellular Biosciences, University of Tokyo, Bunkyo-ku, Tokyo, Japan, [4]SORST, Japan Science and Technology, Kawaguchi, Saitama, Japan and [5]Ankhs Inc., Tsukuba-city, Ibaraki, Japan

Recent evidence indicates that the transactivation of estrogen receptor α (ERα) requires estrogen-dependent receptor ubiquitination and degradation. Here we show that estrogen-unbound (unliganded) ERα is also ubiquitinated and degraded through a ubiquitin–proteasome pathway. To investigate this ubiquitin–proteasome pathway, we purified the ubiquitin ligase complex for unliganded ERα and identified a protein complex containing the carboxyl terminus of Hsc70-interacting protein (CHIP). CHIP preferentially bound to misfolded ERα and ubiquitinated it to induce degradation. Ligand binding to the receptor induced the dissociation of CHIP from ERα. In CHIP−/− cells, the degradation of unliganded ERα was abrogated; however, estrogen-induced degradation was observed to the same extent as in CHIP+/+ cells. Our findings suggest that ERα is regulated by two independent ubiquitin–proteasome pathways, which are switched by ligand binding to ERα. One pathway is necessary for the transactivation of the receptor and the other is involved in the quality control of the receptor.

The EMBO Journal (2004) **23**, 4813–4823. doi:10.1038/sj.emboj.7600472; Published online 11 November 2004
Subject Categories: chromatin & transcription; proteins
Keywords: estrogen receptor; nuclear receptors transcription; ubiquitination

Introduction

The effects of estrogen are mediated through the estrogen receptors ERα and ERβ, which function as ligand-induced transcriptional factors and belong to the nuclear receptor superfamily (Beato *et al*, 1995; Mangelsdorf *et al*, 1995; Chambon, 1996; McKenna and O'Malley, 2002). Estrogen binding to its receptor induces the ligand-binding domain (LBD) to undergo a characteristic conformational change, whereupon the receptor dimerizes, binds to DNA and subsequently stimulates the gene expression. ERα is stimulated by two distinct activation regions, activation function-1 (AF-1) and AF-2, which are located in the C-terminal LBD and exert ligand-dependent transcriptional activity. Cellular response to estrogen is tightly controlled, and a large number of ERα-interacting proteins have been described as coactivators or corepressors that modify ERα transcriptional activity (Shang *et al*, 2000; Yanagisawa *et al*, 2002; Metivier *et al*, 2003).

Crystal-structural analysis of ERα and other nuclear receptors has revealed the presence of 12 conserved helices in their LBD (Shiau *et al*, 1998). The LBD forms a structure described as a sandwich of 12 α-helices (Helices 1–12) with a central hydrophobic ligand-binding pocket. Helix 12, the most C-terminal of these helices, has been identified as the critical core (AD core) of the AF-2 function of the receptor and plays an important role in coactivator binding to the ligand-bound receptor. In the presence of the ligand, the hinge region between Helices 11 and 12 moves closer to Helices 3 and 5, and Helix 12 is positioned over the ligand-binding pocket formed by Helices 3–5. The repositioned Helix 12 forms a hydrophobic groove with Helices 3 and 5. This hydrophobic groove is known to be important for the interaction with LXXLL motifs found in coactivator molecules (Heery *et al*, 1997).

The activation of nuclear receptors appears to be coupled with the degradation of these proteins by the ubiquitin–proteasome pathway (Boudjelal *et al*, 2000; Dace *et al*, 2000; Blanquart *et al*, 2002). Several recent studies have focused on the involvement of the ubiquitin–proteasome pathway in the estrogen-dependent degradation of ERα, which can be blocked with specific inhibitors of proteasome function, such as MG132 and lactacystin. It has also been reported that the 26S proteasome is essential for estrogen-dependent ERα transcription activity (Nawaz *et al*, 1999a; Lonard *et al*, 2000; Reid *et al*, 2003). Furthermore, several components of the ubiquitin–proteasome pathway have been identified as nuclear receptor-interacting proteins, including SUG1/TRIP1 (Lee *et al*, 1995), RSP5/RPF1 (Imhof and McDonnell, 1996), E6-AP (Nawaz *et al*, 1999b) and UBC9 (Poukka *et al*, 1999). These observations suggest that the ubiquitin–proteasome pathway may play an important role in regulating nuclear receptor levels and restricting the duration and magnitude of receptor activity in response to ligands. Nonetheless, mechanisms governing ERα protein levels remain poorly understood.

Here we show that, in the absence of estrogen, ERα is also ubiquitinated and degraded via a ubiquitin–proteasome pathway. The observation that estrogen-dependent ubiquitination of the receptor required the AD core region within the ERαLBD, whereas the ubiquitination of the unliganded receptor did not, raised the possibility that the ubiquitin ligase for unliganded ERα might differ from the ligase involved in estrogen-dependent ubiquitination. Therefore, we purified

*Corresponding author. Graduate School of Life and Environmental Sciences, University of Tsukuba, 1-1-1 Tenno-dai, Tsukuba Science City, Ibaraki 305-8572, Japan. Tel.: +81 29 853 6632; Fax: +81 29 853 4605; E-mail: junny@agbi.tsukuba.ac.jp
[6]These authors contributed equally to this work

Received: 21 June 2004; accepted: 12 October 2004; published online: 11 November 2004

the ubiquitin-ligase complex for unliganded ERα and identified a chaperone complex containing the carboxyl terminus of Hsc70-interacting protein (CHIP) (Ballinger *et al*, 1999; Dai *et al*, 2003). CHIP selectively bound to and ubiquitinated misfolded ERα and stimulated the degradation of these receptors. This model was further supported by an experiment using CHIP-deficient mouse (CHIP−/−) embryonic fibroblast cells. The unliganded ERα was degraded in CHIP+/+ cells but not in CHIP−/− cells under thermally stressed conditions. In contrast, estrogen-dependent degradation was observed in both CHIP+/+ and CHIP−/− cells, supporting the idea that the inactive and active forms of the receptor are regulated by two independent ubiquitin–proteasome pathways. Our findings shed light on the ubiquitin–proteasome network regulating nuclear receptors.

Results

Unliganded ERα is degraded through a ubiquitin–proteasome pathway

As shown in Figure 1A, addition of estrogen to MCF-7 cells reduced the level of ERα protein. The reduction of ERα was inhibited by the proteasome inhibitors MG132 or lactacystin. In the absence of estrogen, MG132 or lactacystin treatment also resulted in ERα accumulation (Figure 1A, lanes 3 and 5), suggesting that not only estrogen-bound ERα but also unliganded ERα is degraded through proteasomes. In ubiquitination assay, ERα was ubiquitinated in both the presence and absence of estrogen (Figure 1B, lanes 3 and 4), indicating that this process is mediated through ubiquitin–proteasome pathways.

We next determined whether the degradation of unliganded and liganded ERα is regulated by the same ubiquitin–proteasome pathway. It has been reported that truncated ERα, ERαΔAD, which does not have an AD core domain, does not exhibit estrogen-dependent degradation (Lonard *et al*, 2000). Thus, we examined the ubiquitination and degradation of ERαΔAD. ERα and ERαΔAD were transfected into 293 cells and the ERα protein level was examined by Western blot analysis. While the ERα degradation was observed regardless of estrogen treatment, ERαΔAD was stabilized by ligand binding, as it accumulates in response to estrogen. MG132 treatment increases the levels of ERαΔAD in the absence of the ligand but does not affect its estrogen-induced accumulation (Figure 1C). We next tested whether ERαΔAD turnover is

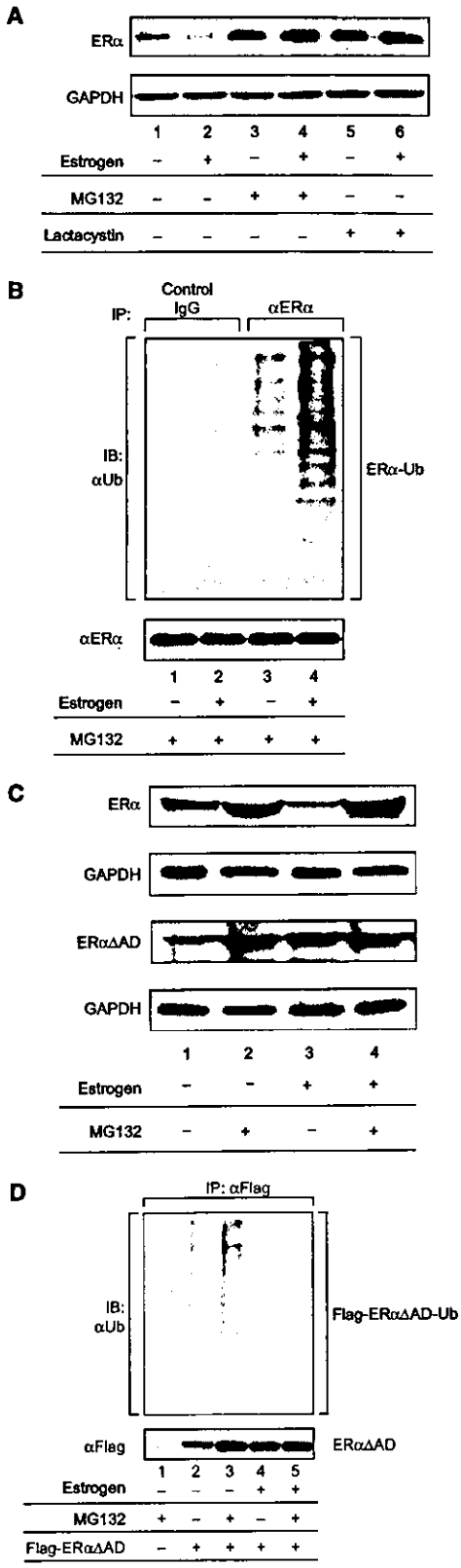

Figure 1 Unliganded ERα was degraded through a ubiquitin–proteasome pathway. (**A**) ERα was degraded in the absence of estrogen. The MCF-7 cells were cultured in the presence or absence of estrogen (10^{-8} M), or the proteasome inhibitor MG132 or lactacystin (10^{-6} M). ERα level was analyzed by Western blotting using anti-ERα monoclonal antibody. (**B**) ERα was ubiquitinated in the absence of estrogen. MCF-7 cells were cultured in the presence or absence of estrogen (10^{-8} M) or MG132 (10^{-6} M). ERα was immunoprecipitated using anti-ERα antibody. The ubiquitination status of ERα was analyzed by Western blotting using anti-ubiquitin antibody. (**C**) ERαΔAD was selectively degraded in the absence of estrogen. 293 cells were transfected with either ERα or ERαΔAD (500 ng). At 24 h post-transfection, the cells were cultured in the presence or absence of estrogen (10^{-8} M) or MG132 (10^{-6} M). ERα or ERαΔAD protein levels were analyzed by Western blotting using anti-ERα antibody. (**D**) ERαΔAD was ubiquitinated in the absence of estrogen. Flag-tagged ERαΔAD (500 ng) was transfected into 293 cells in the presence or absence of estrogen (10^{-8} M) or MG132 (10^{-6} M). Flag-tagged ERαΔAD was immunoprecipitated using anti-Flag M2 antibody. The ubiquitination status of ERαΔAD was analyzed by Western blotting using anti-ubiquitin antibody.

mediated through ubiquitination. In the absence of MG132, we detected almost no or little ubiquitination of ERαΔAD in the presence and absence of estrogen (Figure 1D, lanes 2 and 4). However, in the presence of MG132, we observed smeary bands of ubiquitin-conjugated ERαΔAD products in the absence of estrogen (Figure 1D, lane 3). These results indicate that while ERαΔAD shows no ligand-dependent ubiquitination, unliganded ERαΔAD is still degraded through ubiquitin–proteasome pathways. According to these results, there are possibly two independent ubiquitination pathways for ERα.

Unliganded ERα associates with a protein complex containing CHIP

We then investigated the region responsible for the degradation of unliganded ERα. The protein level of truncated ERα was examined by Western blotting in the presence or absence of estrogen. As shown in Figure 2A, all of the deletion mutants containing the E domain accumulated with estrogen treatment. MG132 treatment increased the levels of these mutants, indicating that they were degraded through proteasome (Figure 2A, lower panel). These results suggest that the region responsible for the degradation of unliganded ERα is located within ERαLBD. From these results, we speculated that an E3 ubiquitin ligase specifically binds and conjugates ubiquitin to the unliganded ERαLBD. We therefore attempted to identify the putative ubiquitin ligase for unliganded ERα. A HeLa cell extract-derived fraction was incubated with glutathione-*S*-transferase (GST)-fused ERαLBD in the presence or absence of estrogen. Proteins that interacted with ERαLBD were separated by SDS–polyacrylamide gel electrophoresis (SDS–PAGE) and silver stained (Figure 2B). To identify the proteins that selectively bound to unliganded ERαLBD, we performed peptide mass fingerprinting, and revealed that the 35 kDa protein eluted from the unliganded ERαLBD column consisted of CHIP (Figure 2B). The result obtained from peptide mass fingerprinting was confirmed by Western blotting using a specific antibody against CHIP (Figure 2B, lower panel).

CHIP is known to possess E3 ubiquitin-ligase activity mediated by its carboxy-terminal U-box domain and has the ability to bind to chaperones Hsp/Hsc70 by means of its tetratricopeptide repeat (TPR) domain (Scheufler *et al*, 2000; Connell *et al*, 2001; Imai *et al*, 2002). Mass spectrometric analysis also identified chaperone proteins Hsp/Hsc70 (Figure 2B), indicating that CHIP binds unliganded ERαLBD as a protein complex containing Hsp/Hsc70. Thus, we examined the interaction between ERα and CHIP/Hsp/Hsc70 complex using a co-immunoprecipitation method. As shown in Figure 2C, CHIP is selectively co-immunoprecipitated with

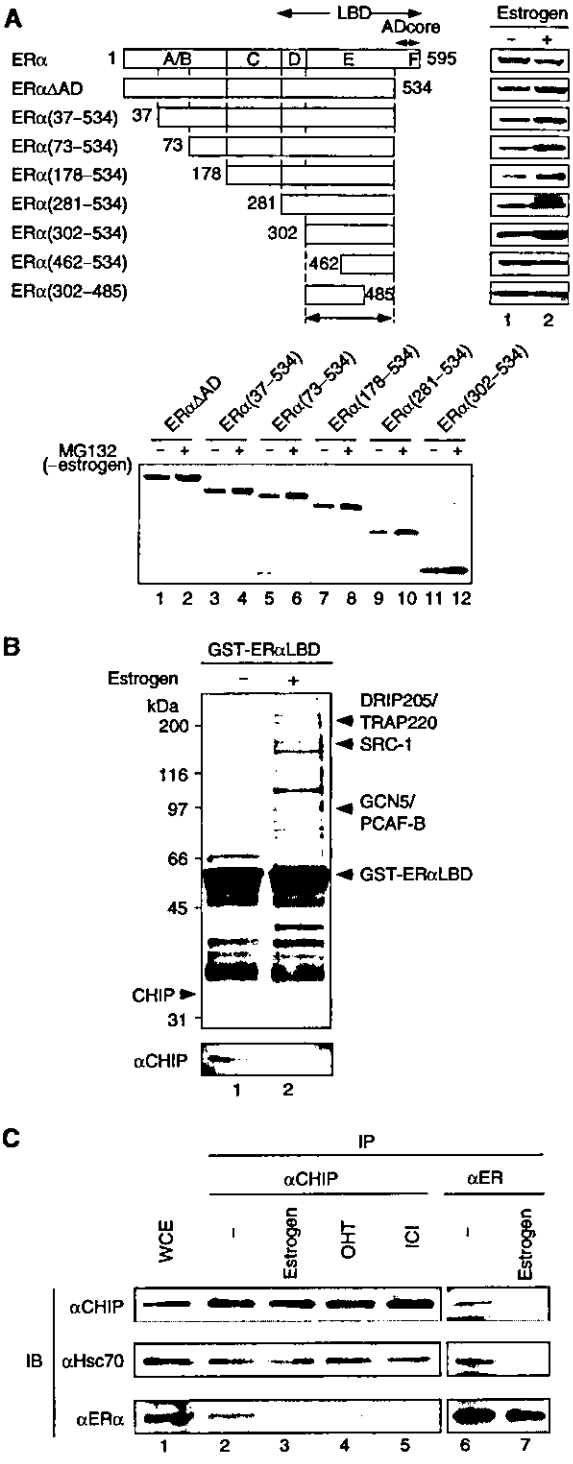

Figure 2 The unliganded ERα associated with a protein complex containing CHIP and Hsc/Hsp70. **(A)** The E region of ERα was sufficient for the degradation of unliganded ERα. Indicated Flag-tagged ERα deletion mutants (500 ng) were transfected into 293 cells. These cells were cultured in the presence or absence of estrogen (10^{-8} M) (upper panel) or MG132 (10^{-6} M) (lower panel). To evaluate the protein level of ERα mutants, Western blot analysis was performed using anti-Flag M2 antibody. **(B)** Purification and identification of ERαLBD-interacting proteins. Extracts prepared from HeLa S3 cells were incubated with immobilized GST-ERαLBD in the presence or absence of estrogen (10^{-6} M). ERα-interacting proteins were eluted from the GST-ERαLBD column by *N*-lauroyl sarkosin and subjected to SDS–PAGE followed by silver staining. The fractions eluted from unliganded GST-ERαLBD column (lane 1) and liganded GST-ERαLBD column (lane 2) are shown. Proteins eluted from both columns were examined by mass spectrometry. *Hsc70. **(C)** Interaction between unliganded ERα and CHIP *in vivo*. MCF-7 cells were lysed and subjected to immunoprecipitation using either anti-CHIP or anti-ERα antibody in the presence or absence of indicated ligands (estrogen (10^{-8} M); OHT: 4-hydroxytamoxifen (10^{-6} M); ICI: ICI182,780 (10^{-7} M)). The precipitates were Western blotted with antibodies for CHIP, ERα and Hsc70. MCF-7 whole-cell extract is shown in lane 1 (WCE).

unliganded ERα and Hsc70. Cell treatment with either 4-hydroxytamoxifen (OHT), a partial antagonist of ERα, or ICI182,780 (ICI), a pure antagonist of ERα, abrogated the binding between ERα and CHIP. CHIP was also detected in the immunoprecipitation performed with an anti-ERα antibody in the absence of ligands, confirming the interaction between ERα and CHIP *in vivo*. The same results were obtained in the human endometrial adenocarcinoma cell line Ishikawa (data not shown).

To better characterize and identify other components of the CHIP–Hsc70 complex, we generated HeLa cell lines stably expressing Flag-HA double-tagged CHIP. The protein complex containing CHIP was precipitated and separated by SDS–PAGE. Protein identification of the purified proteins by mass spectrometric analysis identified KIAA0678, Hsp90, Hsc70, Hsp70, Hsp40 and CHIP (Figure 3A). The protein components of the CHIP complex were confirmed by Western blotting using specific antibodies. Hsp90, Hsc70, Hsp70, Hsp40 and BAG-1 in the CHIP complex are shared with the chaperone components, whereas other chaperone components, Hip, Hop and p23, were undetectable by Western blot analysis (Figure 3B). To investigate whether this protein complex binds to unliganded ERα, Flag-tagged ERα expressed in 293 cells was immunoprecipitated using anti-Flag monoclonal antibody. As shown in Figure 3C, all of the components detected in the CHIP complex by Western blotting existed in the precipitant (Figure 3C, left panel). Next, to investigate whether this protein complex has the same composition in physiological conditions, ERα was immunoprecipitated from MCF-7 cells using a specific antibody for ERα. In the absence of estrogen, the protein complex purified from MCF-7 contained the same components as the complex in 293 cells (Figure 3C, right panel), suggesting that this protein complex exists in the physiological conditions.

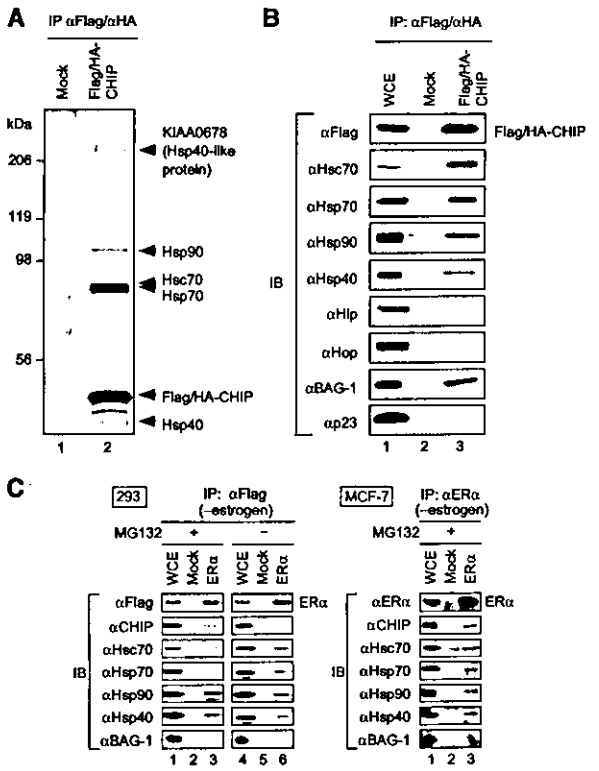

Figure 3 Purification and identification of a protein complex containing CHIP. (**A**, **B**) HeLa S3 cells (Mock) or HeLa S3 cells constitutively expressing Flag/HA double-tagged CHIP (Flag/HA-CHIP) were subjected to sequential immunoprecipitation using anti-Flag M2 and anti-HA antibody as described in Materials and methods. The purified fractions were subjected to SDS-PAGE followed by silver staining (A). Proteins eluted from these columns were examined by mass spectrometry (A) and Western blotting (B). Total HeLa cell extract is shown in lane 1 (WCE) (B). (**C**) Unliganded ERα interacted with a protein complex containing chaperones and CHIP. Flag-ERα-transfected 293 cells (ERα), untransfected cells (Mock) or MCF-7 cells were subjected to immunoprecipitation using either anti-Flag M2 (left panel) or anti-ERα (right panel) antibody and then Western blotted using indicated antibodies. The whole-cell extract is shown in lane 1 (WCE).

CHIP ubiquitinates and degrades unliganded ERα

To test whether CHIP is involved in the ubiquitination and degradation of unliganded ERα, either ERα or ERαΔAD was transfected into 293 cells with or without CHIP. Western blot analysis revealed that, in the absence of estrogen, the steady-state levels of ERα and ERαΔAD were decreased when CHIP was expressed (Figure 4A; 293, lanes 3 and 5). In contrast, in the presence of estrogen, the expression of CHIP exhibited little or no effect on the protein level of ERα and ERαΔAD (Figure 4A; 293, lanes 4 and 6). Endogenous ERα in MCF-7 cells was also decreased by CHIP expression (Figure 4A; MCF-7). Cell treatment with MG132 or lactacystin blocked CHIP-dependent ERα degradation, indicating that the degradation is mediated through proteasome pathways (Figure 4A, lower panel). We further determined the CHIP function by developing MCF-7 cells in which endogenous CHIP expression was suppressed by the introduction of a small interfering RNA (siRNA) complementary to sequences present in the CHIP mRNA. The introduction of the siRNA vector into MCF-7 cells resulted in the suppression of CHIP mRNA (data not shown) and protein expression, and the accumulation of ERα protein (Figure 4B). In contrast, a control vector failed to alter the CHIP or ERα protein level. In addition, either OHT or ICI treatment abrogated CHIP-induced ERα degradation (Figure 4C). Considering the observation that OHT- or ICI-bound ERα showed no interaction with CHIP, it is suggested that the degradation requires binding between ERα and CHIP.

To confirm that CHIP enhances unliganded ERα degradation, pulse-chase experiments were performed. In the absence of CHIP, the half-life of unliganded ERα exceeded 12 h (Figure 4D; 293), whereas, in the presence of CHIP, the turnover of unliganded ERα increased and exhibited a half-life of approximately 6 h (Figure 4D; 293). The half-life of estrogen-bound ERα was not changed by the expression of CHIP (data not shown). In MCF-7 cells, CHIP also enhanced the turnover of endogenous ERα in the absence of estrogen (Figure 4D; MCF-7). To test the specificity of this effect, we created constructs in which the TPR and U-box domains of CHIP were deleted (ΔTPR and ΔUbox). CHIP binds to Hsp/Hsc70 by means of its TPR motif, while also displaying E3 ubiquitin-ligase activity mediated by its U-box domain. Although the expression of these proteins was similar to that of wild-type CHIP (data not shown), the deletion of either of these domains abolished the effects of CHIP on ERα or ERαΔAD protein level (Figure 5A). The requirement of a TPR motif indicates that CHIP may need to interact with Hsc70 to promote ERα degradation. Functional requirement

of the U-box implies that CHIP regulates ERα ubiquitination. In order to validate this model, we evaluated the presence of Hsp/Hsc70 and ERα in complexes containing CHIPΔTPR or CHIPΔUbox. As shown in Figure 5B, CHIPΔTPR did not have the ability to form a complex with Hsc70 and ERα, indicating that Hsc70 mediates the interaction between ERα and CHIP. Finally, we tested whether CHIP enhances ERα turnover through ubiquitination. When ERα was coexpressed with CHIP, we observed the appearance of smeary bands of ubiquitin-conjugated ERα products (Figure 5C, lanes 3 and 5). In the presence of estrogen, CHIP did not enhance the conjugation of ubiquitin to ERα (Figure 5C, lanes 2 and 4). Overall, these observations indicate that the ubiquitination and degradation of unliganded ERα is mediated by a protein complex containing CHIP ubiquitin ligase.

CHIP preferentially recognizes and degrades misfolded ERα

To investigate the effect of CHIP on the transcriptional activity of ERα, a luciferase assay was performed as shown in Figure 6A. While the protein level of ERα was reduced by the expression of CHIP (Figure 6B, upper panel), the transcriptional activity of ERα was slightly enhanced by CHIP expression (Figure 6B, lower panel, compare lane 2 with lanes 5 and 8). Therefore, we next estimated the level of transcriptional activity per ERα protein amount. When ERα was coexpressed with CHIP, the level of transcriptional activity per ERα protein was about two-fold higher than ERα alone (Figure 6B, lower panel, compare lane 3 with lanes 6 and 9).

Our results show that CHIP binds to unliganded but not to liganded ERα. In addition, CHIP was localized mainly in the cytoplasm (Figure 6C). From these observations, it is difficult to believe that CHIP acts as a coactivator for ERα in the nucleus. Furthermore, ERα(HE82), which has three amino-acid substitutions in the DNA-binding region (C domain) in ERα and has almost no ability to bind DNA (Mader *et al*, 1989), was also degraded by CHIP, suggesting that the CHIP-dependent degradation of ERα does not require DNA binding. From these results and previous reports (Hohfeld *et al*, 2001; Meacham *et al*, 2001; Murata *et al*, 2001; Goldberg, 2003), we hypothesized that CHIP preferentially ubiquitinates misfolded ERα proteins to eliminate them. CHIP expression may selectively reduce the protein level of unfolded or misfolded ERα, which has less activity than the normal form. Consequently, CHIP could enhance the level of transcriptional activity per ERα protein.

To test this hypothesis, amino-acid substitutions were introduced into ERα to induce protein misfolding. In the absence of ligands, ERα(V364E) (McInerney *et al*, 1996)

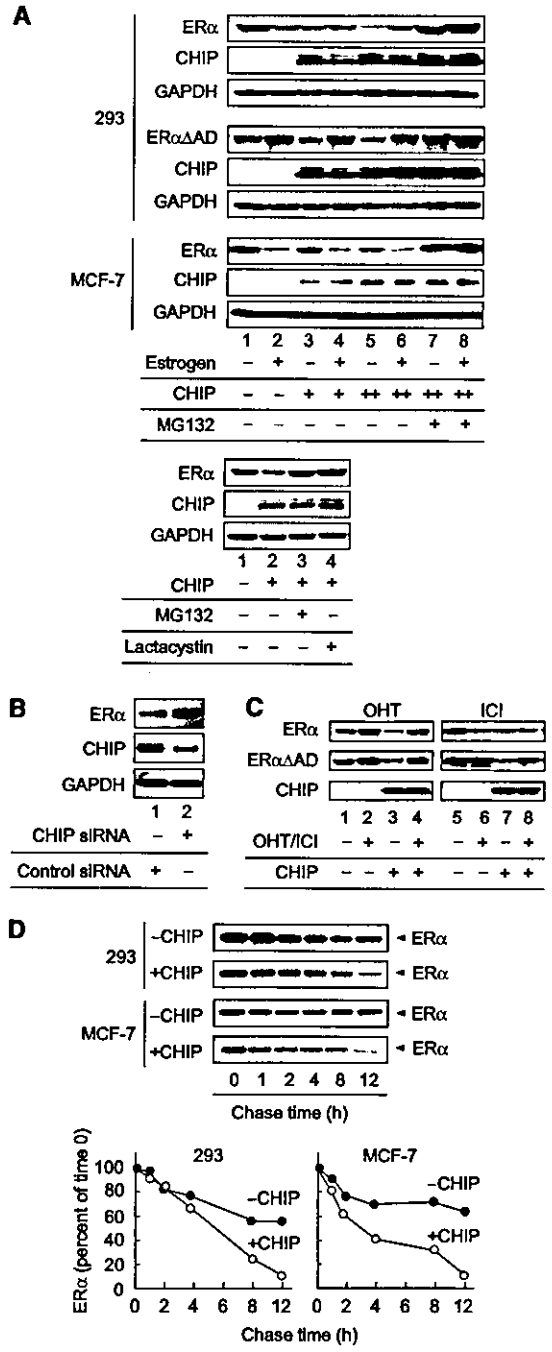

Figure 4 CHIP ubiquitinated and degraded unliganded ERα. **(A)** CHIP facilitated the degradation of unliganded ERα. HA-tagged CHIP (250 ng) was cotransfected into 293 or MCF-7 cells with or without ERα or ERαΔAD (500 ng) and in the absence or presence of estrogen (10^{-8} M), MG132 or lactacystin (10^{-6} M). The protein level of ERα was examined by Western blotting using anti-ERα antibody. **(B)** siRNA-mediated suppression of endogenous CHIP. The plasmid containing siRNA specific for CHIP or control vector was introduced into MCF-7 cells. Transfected cells were selected by puromycin. Protein levels of CHIP and ERα were assessed by immunoblotting of whole-cell lysate with the specific antibodies as indicated. **(C)** CHIP did not alter the steady-state level of ERα in the presence of OHT or ICI. Either ERα or ERαΔAD (500 ng) was cotransfected into 293 cells with or without HA-CHIP (250 ng) in the absence or presence of the indicated ligands. The protein level of ERα was examined by Western blotting using specific antibodies for ERα. **(D)** Pulse-chase assay. 293 cells transfected with CHIP (250 ng) and ERα (500 ng) or MCF-7 cells transfected with CHIP (2 μg) were pulse-labeled with [^{35}S]methionine and then chased for the indicated times in media containing unlabeled methionine. ^{35}S-labeled ERα in anti-ERα immunoprecipitate was quantified by phosphoimaging, and the levels in control cells (closed circle) and CHIP-expressing cells (open circle) were plotted relative to the amount present at time 0.

and ERα(C447A) (Reese and Katzenellenbogen, 1992), both of which have an amino-acid substitution in the LBD and exhibit temperature sensitivity, were unstable and degraded faster than wild-type protein at a nonpermissive temperature (37°C). Wild-type ERα also degraded to the same extent as temperature-sensitive mutants when cells were cultured under thermally stressed conditions (cells were cultured at 42°C for 30 min) (Figure 6D, upper panel, compare lane 1 with lanes 2, 3 and 6). In contrast, ERα(L540Q) (Ince *et al*, 1995) and ERαΔAD, which have either an amino-acid substitution or truncation in the flexible Helix 12 region, exhibited the same stability as wild type at 37°C (Figure 6D, upper panel, compare lane 1 with lanes 4 and 5). Under a permissive temperature (30°C), the protein stability of ERα(V364E) and ERα(C447A) was comparable with that of the wild type (Figure 6D, lower panel).

In a luciferase assay, these four mutated ERα proteins showed a loss or reduction of transcriptional activity compared to the wild type (Figure 6E, lane 5), and they were able to suppress wild-type activity when coexpressed with wild-type ERα (Figure 6E, lane 8). CHIP did not enhance the ERα activity suppressed by ERα(L540Q) or ERαΔAD; however, transcriptional activity suppressed by ERα(V364E) or ERα(C447A) was recovered by CHIP expression (Figure 6E, lanes 9 and 10). These results suggest that CHIP may preferentially ubiquitinate ERα(V364E) and ERα(C447A) to degrade these mutants.

If CHIP is directly involved in the hydrolysis of abnormal or mutant forms of ERα, then it should be able to form specific complexes with mutated or misfolded ERα. ERα or mutated forms of ERα were immunoprecipitated from transfected cells and the presence of CHIP and chaperone proteins was detected using specific antibodies. At a permissive temperature (30°C), the amount of CHIP in the precipitate pellets with ERα(V364E) or ERα(C447A) was almost the same in precipitates with the wild type (Figure 7A, right panel). However, at a nonpermissive temperature (37°C), CHIP and BAG-1, a co-chaperone that binds to both Hsc70 and the proteasome, preferentially co-immunoprecipitated with ERα(V364E) and ERα(C447A), while the amount of other chaperone components in precipitants was unchanged (Figure 7A, left panel). In addition, thermally stressed conditions (42°C for 30 min) also increased the CHIP and BAG-1 levels in the precipitated pellet (Figure 7A, left panel, lane 6). Consistent with the results obtained from the degradation and interaction experiments, the polyubiquitination of the temperature-sensitive mutants or thermally denatured ERα was enhanced at nonpermissive temperature (Figure 7B, compare left panel with right panel).

Liganded but not unliganded ERα degradation is observed in CHIP−/− cells

To firmly establish the importance of the observation of CHIP-dependent ERα degradation, we isolated mouse embryonic

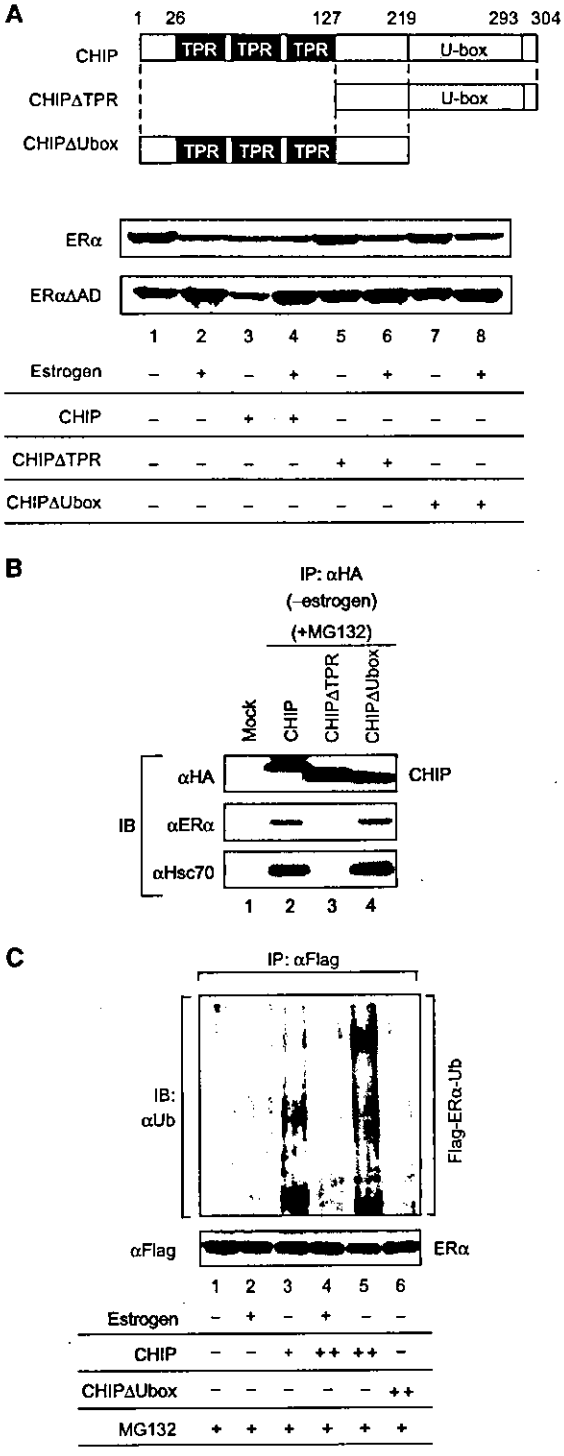

Figure 5 CHIP-dependent ubiquitination and degradation of ERα required its TPR and U-box domain. (**A**) Both the TPR and U-box domain in CHIP were necessary for ERα degradation. CHIP, CHIPΔTPR or CHIPΔUbox (250 ng) was transfected into 293 cells with or without ERα or ERαΔAD (500 ng). Protein levels of ERα and ERαΔAD were examined by Western blotting using anti-ERα antibody. (**B**) The TPR domain of CHIP is necessary for binding to Hsc70 and ERα. HA-tagged CHIP or CHIP mutants were expressed in 293 cells and immunoprecipitated with anti-HA antibody in the absence of estrogen. Precipitates were Western blotted with antibodies for CHIP, ERα and Hsc70. (**C**) CHIP induced the ubiquitination of unliganded ERα. Flag-tagged ERα (500 ng) was transfected into 293 cells with or without CHIP (250 ng) or CHIPΔUbox (250 ng) in the presence or absence of estrogen (10^{-8} M). Flag-tagged ERα was immunoprecipitated using anti-Flag M2 antibody. The ubiquitination status of ERα was analyzed by Western blotting using anti-ubiquitin antibody.

fibroblast (MEF) cells from either CHIP−/−, CHIP+/− mice or wild-type littermates, CHIP+/+, and determined the protein level of ERα. To induce misfolding of ERα protein, these cells were cultured under thermally stressed conditions. In the absence of estrogen, the thermally stress conditions reduced ERα levels in both CHIP+/+ and CHIP+/− cells but not in CHIP−/− cells (Figure 8A, lanes 4–6). MG132 induced the accumulation of ERα in CHIP+/+ and CHIP+/− cells, indicating that ERα was degraded through proteasome pathways in these cells. These observations provide further support for a model in which CHIP preferentially binds misfolded ERα proteins and degrades them to maintain the quality of ERα protein in cells. Co-immunoprecipitation experiments showed the existence of ERα/Hsc70/CHIP complex in CHIP+/+ cells but not in CHIP−/− cells (Figure 8B). Furthermore, estrogen treatment induced ERα degradation in CHIP−/− cells to the same extent as in CHIP+/+ cells (Figure 8C), suggesting that CHIP is not involved in estrogen-dependent degradation, and supporting the idea that there are two independent ubiquitin–proteasome pathways for ERα (Figure 8D).

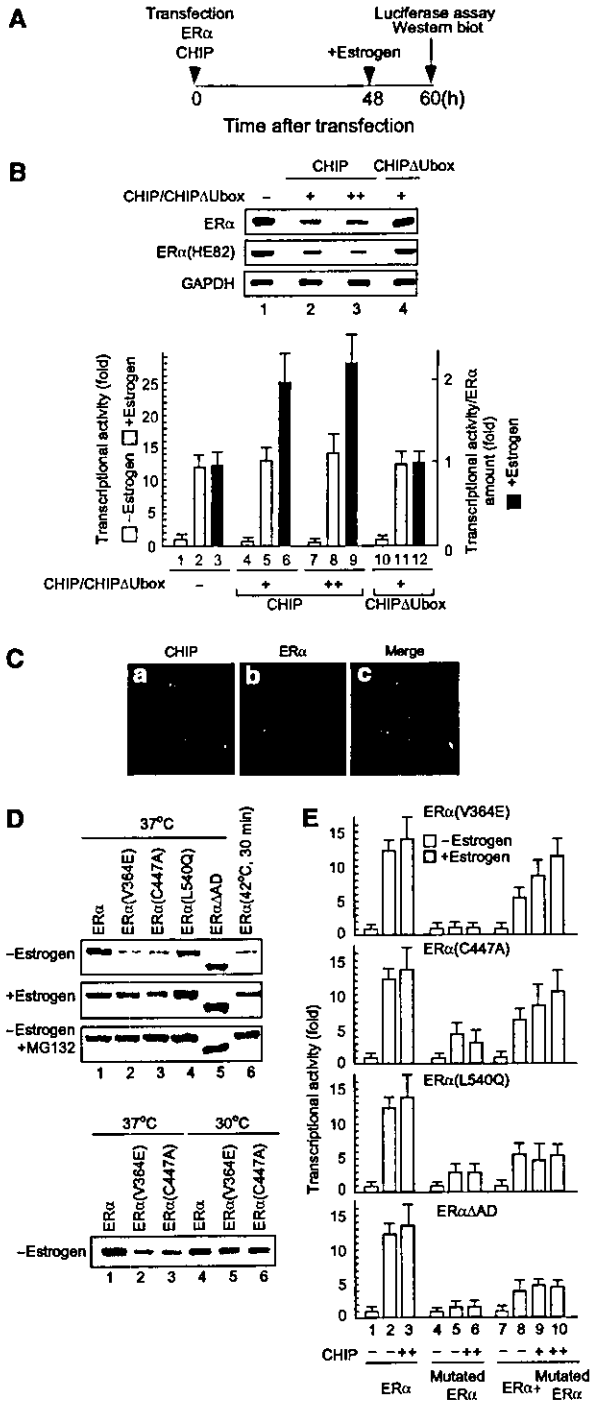

Figure 6 CHIP preferentially recognized and degraded misfolded ERα. (**A**) The time schedule for luciferase assay and Western blot analysis. 293 cells were transfected with indicated plasmids. At 48 h after transfection, cells were treated with estrogen (10^{-8} M) for an additional 12 h and harvested for luciferase assay and Western blotting. (**B**) The level of transcriptional activity per ERα protein amount was enhanced by CHIP. Upper panel: The steady-state level of ERα or ERα(HE82) was reduced by the expression of CHIP but not by CHIPΔUbox. Lower panel: Transcriptional activity of ERα was slightly enhanced by CHIP. ERα (100 ng) and either CHIP or CHIPΔUbox (100 ng) were cotransfected into 293 cells with ERE-TATA-Luc (100 ng) and pRSVβGAL (100 ng), and cell extracts were used in a luciferase assay. The protein amount of ERα was quantified by phosphoimaging. The levels of transcriptional activity per ERα protein amount were plotted relative to the level in control cells. (**C**) Immunocytochemistry of CHIP and ERα. 293 cells were transiently transfected with HA-tagged CHIP and ERα. The mounted cells were examined by immunofluorescence microscopy as described in Materials and methods. Green represents immunofluorescence for HA-CHIP and red ERα. The distribution of CHIP in a cell body is shown in panel a, and panel b shows the distribution of ERα. Panel c shows the merge images of panels a and b. (**D**) Temperature-sensitive mutants of ERα degraded faster than wild-type ERα in the absence of ligands. ERα(V364E), ERα(C447A), both of which are temperature sensitive, and ERα(L540Q) were generated by amino-acid substitutions of wild-type ERα. Indicated ERα or ERα mutants (500 ng) were transfected into 293 cells in the presence or absence of estrogen (10^{-8} M) and MG132 (10^{-6} M) at 30°C (permissive temperature; lower panel), 37°C (normal/nonpermissive temperature; upper panel) or under thermally stressed conditions (42°C for 30 min; upper panel). Protein levels of ERα or mutants were analyzed by Western blotting using anti-ERα antibody. (**E**) CHIP recovered the transcriptional activity of ERα suppressed by coexpression of ERα mutants. ERα (100 ng), ERE-TATA-Luc (100 ng) and pRSVβGAL (100 ng) were cotransfected into 293 cells with or without either ERα(V364E), ERα(C447A), ERα(L540Q), ERαΔAD (100 ng) or CHIP (100 ng), and cell extracts were used in a luciferase assay.

Discussion

Estrogen receptor α is regulated by two independent ubiquitin–proteasome pathways

Several studies have mentioned that the AD core region of ERα is essential not only for transactivation but also for estrogen-dependent ERα degradation (Lonard *et al*, 2000). These reports are in good agreement with our result that ERαΔAD, which has no AD core region, does not show estrogen-dependent degradation. Interestingly, however, MG132 had no effect on ligand-bound ERαΔAD; the steady-state level of ERαΔAD in the absence of estrogen is accumulated in the presence of MG132. These results indicate that unliganded ERαΔAD is still degraded through proteasome pathways. According to these observations, it is possible that the degradation pathway for the unliganded receptor differs from that for liganded. ERαΔAD might be able to recruit a

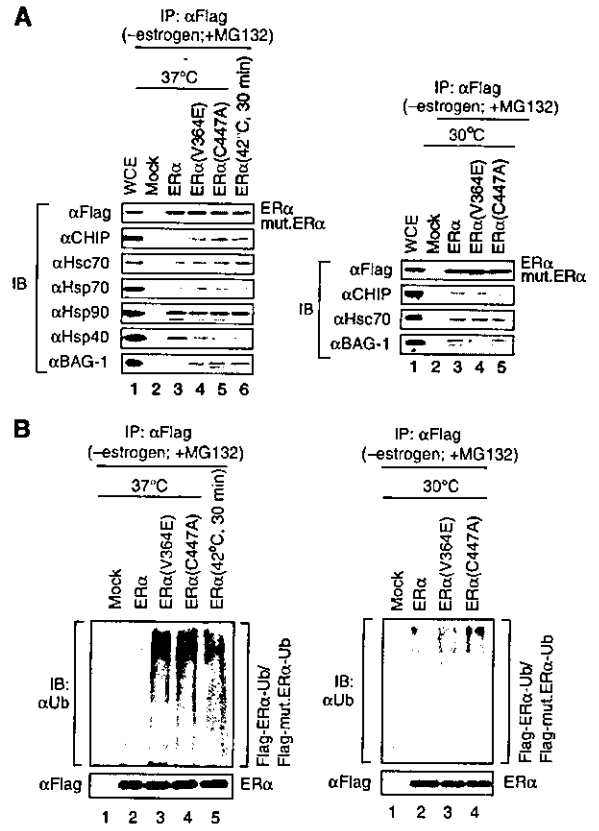

Figure 7 The misfolding of ERα induced the recruitment of CHIP and BAG-1 to the complex. (**A**) CHIP and BAG-1 preferentially recognized and bound misfolded ERα. Flag-tagged ERα, ERα(V364E) or ERα(C447A) (100 ng) was transfected into 293 cells. These cells were cultured with MG132 (10^{-6} M) at 30°C (permissive temperature; right panel), 37°C (normal/nonpermissive temperature; left panel) or under thermally stressed conditions (42°C for 30 min; left panel). Extracts prepared from these cells (lanes 3–6) or untransfected cells (Mock) were subjected to immunoprecipitation using anti-Flag M2 antibody and then Western blotted using antibodies as indicated. The whole-cell extract is shown in lane 1 (WCE). (**B**) The ubiquitination status of the temperature-sensitive mutants or heat-shocked ERα was enhanced. Flag-tagged ERα, ERα(V364E) or ERα(C447A) (500 ng) was transfected into 293 cells. These cells were cultured with MG132 (10^{-6} M) at 30°C (right panel), 37°C (left panel) or under thermally stressed conditions (42°C for 30 min; left panel). Extracts prepared from these cells (lanes 2–5) or untransfected cells (Mock) were subjected to immunoprecipitation using anti-Flag M2 antibody. The ubiquitination status of ERα and mutants was analyzed by Western blotting using anti-ubiquitin antibody.

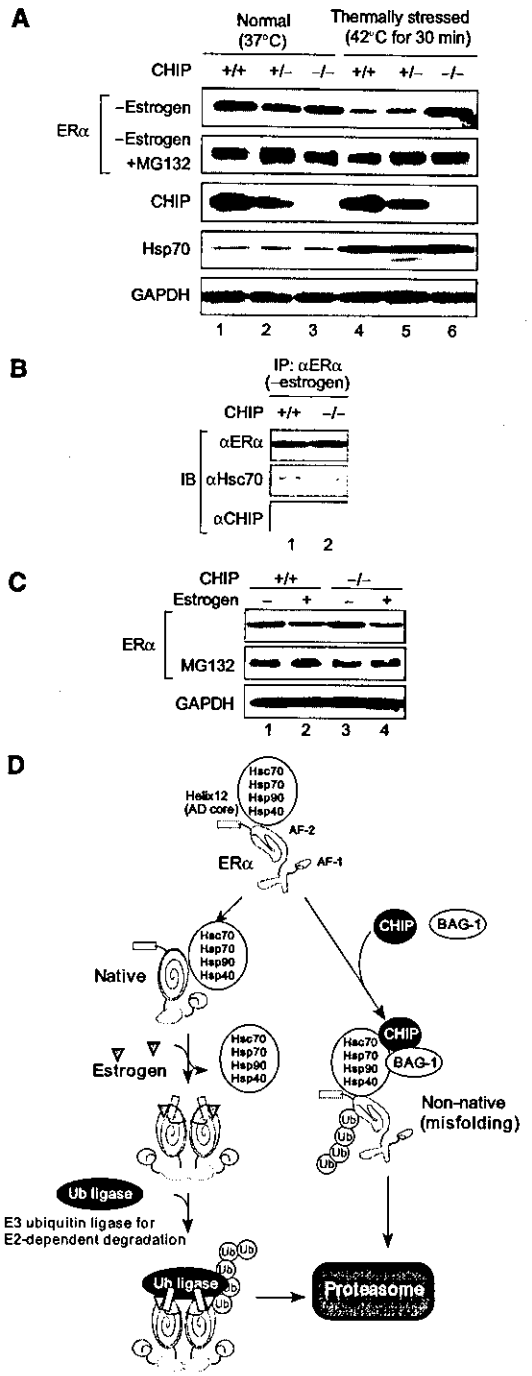

Figure 8 Liganded but not unliganded ERα degradation was observed in CHIP–/– MEF cells. (**A**) Thermally induced degradation of ERα was not observed in CHIP–/– cells. MEF cells were isolated from CHIP–/–, CHIP+/– mice and wild-type littermates (CHIP+/+). MEF cells were cultured under normal conditions (37°C) or thermally stressed conditions (42°C for 30 min) without estrogen. Extracts prepared from the MEF cells were subjected to Western blotting using the indicated antibody. (**B**) CHIP+/+ or CHIP–/– cells were lysed and subjected to immunoprecipitation using anti-ERα antibody in the absence of estrogen. Precipitates were Western blotted with antibodies for ERα, Hsc70 and CHIP. (**C**) Estrogen induced degradation of ERα in CHIP–/– cells. MEF cells were cultured in the presence or absence of estrogen (10^{-8} M), and cell extracts prepared from these cells were subjected to Western blotting using anti-ERα antibody. (**D**) ERα degradation may be regulated by two independent ubiquitin–proteasome pathways.

degradation machinery for the unliganded receptor but not for the liganded. Otherwise, there may be a change in the conformation of the receptor, which would protect the receptor from degradation. Reid *et al* (2003) also demonstrated that unliganded ERα is subject to proteasome-mediated turnover, which is mechanistically different from the turnover of liganded ERα.

Several lines of evidence indicate that estrogen, progesterone and glucocorticoid receptors (GRs) are degraded in the presence of their cognate ligands (Nawaz *et al*, 1999a; Wallace and Cidlowski, 2001). However, this is contrasted with observations of androgen and vitamin D receptors, which are accumulated in the presence of their agonist

ligands (Li *et al*, 1999). From our results, these inconsistent observations might be explained by the balance between the two degradation pathways in the cells. When the degradation pathway for unliganded receptors is more active than that for liganded receptors, these receptors would stabilize in the presence of ligands. In contrast, when the liganded receptor degradation pathway is stronger than the unliganded receptor degradation pathway, the protein level of receptors is down-regulated by ligand treatment.

CHIP containing a protein complex specifically binds and ubiquitinates unliganded estrogen receptor

To address the mechanism of the ubiquitination and degradation of unliganded ERα, we purified proteins using GST-fused ERαLBD, and identified CHIP, which specifically bound to unliganded ERαLBD. Our findings indicate that CHIP binds unliganded ERα as a protein complex containing Hsp90, Hsc70, Hsp70, Hsp40 and BAG-1, all of which are known to possess or assist chaperoning functions, and a Dna J-like protein, KIAA0678. Dna J is a member of the Hsp40 family of molecular chaperones, which regulate the activity of Hsp70s. Dna J-like proteins that contain regions closely resembling a Dna J domain are suggested to regulate the activity of Dna J proteins during protein translocation, assembly and disassembly (Cheetham and Caplan, 1998).

CHIP expression with ERα enhanced the conjugation of ubiquitin to the receptors and stimulated degradation. Receptor ubiquitination and degradation was abrogated when cells were treated with estrogen. These results are in good agreement with the results obtained from binding experiments. Furthermore, OHT and ICI, both of which inhibited the interaction between CHIP and ERα, reduced the CHIP-mediated degradation of ERα. These findings confirmed the idea that unliganded ERα ubiquitination is mediated by CHIP. In immunostaining, CHIP was largely detected in the cytoplasm (Figure 6C). The localization of CHIP was not changed when cells were cultured under heat-stressed conditions (data not shown). According to these results, CHIP-dependent ERα ubiquitination may occur mainly in the cytoplasm. However, we cannot exclude the possibility that a small amount of CHIP is involved in the ubiquitination of ERα in the nucleus.

Recently, CHIP was reported to induce ubiquitination of the GR bound to Hsp90 for proteasomal degradation (Connell *et al*, 2001). While our findings indicate that CHIP selectively binds to unliganded ERα and ubiquitinates it, CHIP-mediated GR degradation is observed in the presence of ligands. Recent reports indicate that in the presence of ligands, nuclear receptors do not remain permanently bound at a promoter, but rather undergo cycles of binding and unbinding (Shang *et al*, 2000; Stenoien *et al*, 2001; Galigniana *et al*, 2004). The cycling of ligand-bound ERα requires proteasomal activity (Reid *et al*, 2003). Together with these reports and our observations, it is possible that the binding of estrogen to ERα induces the dissociation of CHIP and the association of other ubiquitin ligases, which are involved in receptor cycling at a promoter. The ligand-dependent cycling of GR is known to be much faster than that of ERα and both chaperones and proteasomes are thought to be important for GR cycling since the disruption of either leads to alterations in the exchange rate (Galigniana *et al*, 2004). According to these results, it is possible that, while the chaperone complex containing CHIP mainly resides in the cytoplasm, it may translocate into the nucleus and regulate the cycling of liganded GR.

CHIP is involved in the quality control of estrogen receptor

Since CHIP selectively bound to and ubiquitinated unliganded ERα, CHIP seemed not to be directly involved in transcriptional regulation. Recently, it was shown that CHIP is involved in the ubiquitination of the immature cystic fibrosis transmembrane conductance regulator (CFTR) in the endoplasmic reticulum-associated degradation (ERAD) pathway (Wickner *et al*, 1999; Meacham *et al*, 2001). Based on these findings, it is speculated that CHIP may be a new category of E3 enzyme responsible for the quality control of cellular proteins linked to the function of molecular chaperones. However, there is no experimental evidence to show that CHIP indeed acts as E3 ubiquitin ligase capable of distinguishing the non-native states from native states of target proteins *in vivo*.

In this study, we have shown that temperature-sensitive mutants of ERα preferentially recruited CHIP to ubiquitinate and degrade these receptors under nonpermissive temperatures. In addition, the ubiquitination and degradation of unliganded ERα was enhanced when cells were cultured under thermally stressed conditions. These observations suggest that CHIP preferentially induces the hydrolysis of abnormal or mutant forms. Using MEF cells derived from CHIP−/− or wild-type littermates, we confirmed the importance of the observation of CHIP-mediated unfolded ERα degradation. These observations provide direct *in vivo* evidence that CHIP selectively ubiquitinated thermally denatured ERα. Our observations provide the first *in vivo* evidence that CHIP functions as 'quality-control E3' involved in the selective ubiquitination of target proteins by recognizing the non-native state in a molecular chaperone-assisted manner. Furthermore, estrogen treatment induced the degradation of ERα in CHIP−/− cells to the same extent as in CHIP+/+ cells, suggesting that CHIP is not involved in estrogen-dependent degradation, and supporting the idea that there are two independent ubiquitin–proteasome pathways for ERα. Considering that nuclear receptors have conserved LBDs and that some are known to associate with a chaperone complex, our findings raise the possibility that other members of the nuclear receptor family may also be regulated by two independent ubiquitin–proteasome pathways.

Materials and methods

Expression vectors, antibodies, cell culture and transfection

These are available as Supplementary data at *The EMBO Journal* Online.

Co-immunoprecipitation and Western blotting

293 cells were transfected with the indicated plasmids, lysed in TNE (10 mM Tris–HCl (pH 7.8), 1% NP-40, 0.15 M NaCl, 1 mM EDTA, 1 μM phenylmethylsulfonyl fluoride (PMSF), 1 μg/ml aprotinin) buffer. Extracted proteins were immunoprecipitated with the antibody-coated protein A/G Sepharose (Amersham) or anti-Flag M2 agarose (Sigma). The bound proteins were separated by SDS–PAGE, transferred onto polyvinylidine difluoride membranes (Millipore) and detected with indicated antibodies, and secondary antibodies conjugated with horseradish peroxidase. Specific proteins were detected using enhanced chemiluminescence (ECL) Western blot detection system (Amersham).

Ubiquitination assay

MCF7 and 293 cells, which were transfected with or without Flag-tagged ERα and HA-tagged CHIP, were lysed with radioimmunoprecipitation (RIPA) buffer (50 mM Tris–HCl (pH 7.5), 150 mM NaCl, 1% Nonidet P-40, 0.5% sodium deoxycholate, 0.1% SDS) supplemented with COMPLETE protease inhibitor mixture (Roche) and kept for 20 min on ice. The extracts clarified by centrifugation were immunoprecipitated with anti-Flag agarose for 1 h at 4°C. After washing the resin with RIPA buffer, the bound proteins were eluted by incubation for 1 h at 4°C with Flag peptide in RIPA buffer (0.4 mg/ml). Immunoprecipitates were immunoblotted with the indicated antibody.

Protein purification

Immobilized GST-ERαLBD fusion proteins were preincubated for 1 h at 4°C in GST-binding buffer (20 mM Tris–HCl (pH 7.9), 180 mM KCl, 0.2 mM EDTA, 0.5 mM PMSF, 1 mM DTT) containing BSA (1 mg/ml) with or without estrogen (10^{-6} M). Bead-immobilized proteins were then incubated at 4°C for 6–10 h with HeLa cell extracts in the presence or absence of 10^{-6} M estrogen. After washing with GST buffer (GST-binding buffer with 0.1% NP-40) three times, the beads were further washed with GST buffer containing 0.2% *N*-lauroyl sarkosine. Proteins bound to ERα were eluted with 15 mM reduced glutathione in elution buffer (50 mM Tris–HCl (pH 8.3), 150 mM KCl, 0.5 mM EDTA, 0.5 mM PMSF, 5 mM NaF, 0.08% NP-40, 0.5 mg/ml BSA, 10% glycerol). For purification of the Flag/HA-CHIP complex, HeLa cells stably expressing Flag/HA-CHIP were extracted with TNE buffer and extracted proteins were incubated with anti-Flag M2 agarose for 2 h at 4°C. After washing the resin with TNE buffer, the bound proteins were eluted by incubation for 1 h at 4°C with Flag peptide in TNE buffer (0.4 mg/ml). For further purification, eluted fractions were incubated with anti-HA agarose for 2 h at 4°C. After washing with TNE buffer, the bound proteins were eluted with a small aliquot of HA peptide in TNE buffer (0.05 mg/ml).

Pulse chase

MCF7 and 293 cells were transfected with or without ERα and CHIP, and 48 h post-transfection, the cells were labeled for 30 min at 37°C with 50 μCi [^{35}S]methionine per ml in methionine-free Dulbecco's modified Eagle's medium (DMEM). The cells were then washed twice and incubated in DMEM containing 10% FBS for the indicated time periods (chase). At each time point of the chase, cell lysates were immunoprecipitated with anti-ERα antibody. The immunoprecipitates were resolved by SDS–PAGE and visualized by autoradiography. Phosphoimager was used to quantify the metabolically labeled ERα present at each time point.

Immunofluorescence

The 293 cells were grown on poly-L-lysine-coated eight-well chamber culture slides, and transfected with plasmids. At 24 h post-transfection, the cells were fixed with 4% paraformaldehyde in PBS for 10 min and permeabilized with Triton buffer (50 mM Tris–HCl (pH 7.5), 0.5% Triton X-100, 150 mM NaCl, 2 mM EDTA) for 15 min. The cells in each well were blocked with PBS containing 1% BSA and 0.5% goat serum for 3 h at 37°C. The cells were incubated with anti-HA and ERα antibody in PBS containing 1% BSA for 2 h at 37°C. After washing with PBS, the cells were incubated with Alexa fluor 488 goat anti-rat IgG and Alexa fluor 594 goat anti-mouse IgG (Molecular Probes) for 1 h at 37°C and washed with PBS. The sample was mounted in VECTASHIELD mounting medium (Vecter Labs) and analyzed with Leica TCS SP2 spectral confocal scanning system.

RNAi

MCF7 cells maintained in the DMEM medium containing charcoal-stripped FBS were cotransfected with CHIP siRNA vector or luciferase siRNA vector (control) and pUC19 vector carrying puromycin-resistant gene. At 24 h post-transfection, the transfected cells were changed to the medium containing 1 μg/ml of puromycin. At 48 h after puromycin selection, the puromycin-resistant cells were harvested and lysed with TNE buffer. The equal amounts of extracted protein were subjected to Western blotting.

Supplementary data

Supplementary data are available at *The EMBO Journal* Online.

Acknowledgements

We thank Dr Akiyoshi Fukamizu and his laboratory staff for providing materials and instruments. This work was supported by the 21st Century COE Program from the Ministry of Education, Culture, Sports, Sciences, and Technology (MEXT).

References

Ballinger CA, Connell P, Wu Y, Hu Z, Thompson LJ, Yin LY, Patterson C (1999) Identification of CHIP, a novel tetratricopeptide repeat-containing protein that interacts with heat shock proteins and negatively regulates chaperone functions. *Mol Cell Biol* **19**: 4535–4545

Beato M, Herrlich P, Schutz G (1995) Steroid hormone receptors: many actors in search of a plot. *Cell* **83**: 851–857

Blanquart C, Barbier O, Fruchart JC, Staels B, Glineur C (2002) Peroxisome proliferator-activated receptor alpha (PPARalpha) turnover by the ubiquitin–proteasome system controls the ligand-induced expression level of its target genes. *J Biol Chem* **277**: 37254–37259

Boudjelal M, Wang Z, Voorhees JJ, Fisher GJ (2000) Ubiquitin/proteasome pathway regulates levels of retinoic acid receptor gamma and retinoid X receptor alpha in human keratinocytes. *Cancer Res* **60**: 2247–2252

Chambon P (1996) A decade of molecular biology of retinoic acid receptors. *FASEB J* **10**: 940–954

Cheetham ME, Caplan AJ (1998) Structure, function and evolution of DnaJ: conservation and adaptation of chaperone function. *Cell Stress Chaperones* **3**: 28–36

Connell P, Ballinger CA, Jiang J, Wu Y, Thompson LJ, Hohfeld J, Patterson C (2001) The co-chaperone CHIP regulates protein triage decisions mediated by heat-shock proteins. *Nat Cell Biol* **3**: 93–96

Dace A, Zhao L, Park KS, Furuno T, Takamura N, Nakanishi M, West BL, Hanover JA, Cheng S (2000) Hormone binding induces rapid proteasome-mediated degradation of thyroid hormone receptors. *Proc Natl Acad Sci USA* **97**: 8985–8990

Dai Q, Zhang C, Wu Y, McDonough H, Whaley RA, Godfrey V, Li HH, Madamanchi N, Xu W, Neckers L, Cyr D, Patterson C (2003) CHIP activates HSF1 and confers protection against apoptosis and cellular stress. *EMBO J* **22**: 5446–5458

Galigniana MD, Harrell JM, Housley PR, Patterson C, Fisher SK, Pratt WB (2004) Retrograde transport of the glucocorticoid receptor in neurites requires dynamic assembly of complexes with the protein chaperone hsp90 and is linked to the CHIP component of the machinery for proteasomal degradation. *Brain Res Mol Brain Res* **123**: 27–36

Goldberg AL (2003) Protein degradation and protection against misfolded or damaged proteins. *Nature* **426**: 895–899

Heery DM, Kalkhoven E, Hoare S, Parker MG (1997) A signature motif in transcriptional co-activators mediates binding to nuclear receptors. *Nature* **387**: 733–736

Hohfeld J, Cyr DM, Patterson C (2001) From the cradle to the grave: molecular chaperones that may choose between folding and degradation. *EMBO Rep* **2**: 885–890

Imai Y, Soda M, Hatakeyama S, Akagi T, Hashikawa T, Nakayama KI, Takahashi R (2002) CHIP is associated with Parkin, a gene responsible for familial Parkinson's disease, and enhances its ubiquitin ligase activity. *Mol Cell* **10**: 55–67

Imhof MO, McDonnell DP (1996) Yeast RSP5 and its human homolog hRPF1 potentiate hormone-dependent activation of transcription by human progesterone and glucocorticoid receptors. *Mol Cell Biol* **16**: 2594–2605

Ince BA, Schodin DJ, Shapiro DJ, Katzenellenbogen BS (1995) Repression of endogenous estrogen receptor activity in MCF-7 human breast cancer cells by dominant negative estrogen receptors. *Endocrinology* **136**: 3194–3199

Lee JW, Ryan F, Swaffield JC, Johnston SA, Moore DD (1995) Interaction of thyroid-hormone receptor with a conserved transcriptional mediator. *Nature* **374:** 91–94

Li XY, Boudjelal M, Xiao JH, Peng ZH, Asuru A, Kang S, Fisher GJ, Voorhees JJ (1999) 1,25-Dihydroxyvitamin D3 increases nuclear vitamin D3 receptors by blocking ubiquitin/proteasome-mediated degradation in human skin. *Mol Endocrinol* **13:** 1686–1694

Lonard DM, Nawaz Z, Smith CL, O'Malley BW (2000) The 26S proteasome is required for estrogen receptor-alpha and coactivator turnover and for efficient estrogen receptor-alpha transactivation. *Mol Cell* **5:** 939–948

Mader S, Kumar V, de Verneuil H, Chambon P (1989) Three amino acids of the oestrogen receptor are essential to its ability to distinguish an oestrogen from a glucocorticoid-responsive element. *Nature* **338:** 271–274

Mangelsdorf DJ, Thummel C, Beato M, Herrlich P, Schutz G, Umesono K, Blumberg B, Kastner P, Mark M, Chambon P, Evans RM (1995) The nuclear receptor superfamily: the second decade. *Cell* **83:** 835–839

McInerney EM, Ince BA, Shapiro DJ, Katzenellenbogen BS (1996) A transcriptionally active estrogen receptor mutant is a novel type of dominant negative inhibitor of estrogen action. *Mol Endocrinol* **10:** 1519–1526

McKenna NJ, O'Malley BW (2002) Combinatorial control of gene expression by nuclear receptors and coregulators. *Cell* **108:** 465–474

Meacham GC, Patterson C, Zhang W, Younger JM, Cyr DM (2001) The Hsc70 co-chaperone CHIP targets immature CFTR for proteasomal degradation. *Nat Cell Biol* **3:** 100–105

Metivier R, Penot G, Hubner MR, Reid G, Brand H, Kos M, Gannon F (2003) Estrogen receptor-alpha directs ordered, cyclical, and combinatorial recruitment of cofactors on a natural target promoter. *Cell* **115:** 751–763

Murata S, Minami Y, Minami M, Chiba T, Tanaka K (2001) CHIP is a chaperone-dependent E3 ligase that ubiquitylates unfolded protein. *EMBO Rep* **2:** 1133–1138

Nawaz Z, Lonard DM, Dennis AP, Smith CL, O'Malley BW (1999a) Proteasome-dependent degradation of the human estrogen receptor. *Proc Natl Acad Sci USA* **96:** 1858–1862

Nawaz Z, Lonard DM, Smith CL, Lev-Lehman E, Tsai SY, Tsai MJ, O'Malley BW (1999b) The Angelman syndrome-associated protein, E6-AP, is a coactivator for the nuclear hormone receptor superfamily. *Mol Cell Biol* **19:** 1182–1189

Poukka H, Aarnisalo P, Karvonen U, Palvimo JJ, Janne OA (1999) Ubc9 interacts with the androgen receptor and activates receptor-dependent transcription. *J Biol Chem* **274:** 19441–19446

Reese JC, Katzenellenbogen BS (1992) Characterization of a temperature-sensitive mutation in the hormone binding domain of the human estrogen receptor. Studies in cell extracts and intact cells and their implications for hormone-dependent transcriptional activation. *J Biol Chem* **267:** 9868–9873

Reid G, Hubner MR, Metivier R, Brand H, Denger S, Manu D, Beaudouin J, Ellenberg J, Gannon F (2003) Cyclic, proteasome-mediated turnover of unliganded and liganded ERalpha on responsive promoters is an integral feature of estrogen signaling. *Mol Cell* **11:** 695–707

Scheufler C, Brinker A, Bourenkov G, Pegoraro S, Moroder L, Bartunik H, Hartl FU, Moarefi I (2000) Structure of TPR domain-peptide complexes: critical elements in the assembly of the Hsp70–Hsp90 multichaperone machine. *Cell* **101:** 199–210

Shang Y, Hu X, DiRenzo J, Lazar MA, Brown M (2000) Cofactor dynamics and sufficiency in estrogen receptor-regulated transcription. *Cell* **103:** 843–852

Shiau AK, Barstad D, Loria PM, Cheng L, Kushner PJ, Agard DA, Greene GL (1998) The structural basis of estrogen receptor/coactivator recognition and the antagonism of this interaction by tamoxifen. *Cell* **95:** 927–937

Stenoien DL, Patel K, Mancini MG, Dutertre M, Smith CL, O'Malley BW, Mancini MA (2001) FRAP reveals that mobility of oestrogen receptor-alpha is ligand- and proteasome-dependent. *Nat Cell Biol* **3:** 15–23

Wallace AD, Cidlowski JA (2001) Proteasome-mediated glucocorticoid receptor degradation restricts transcriptional signaling by glucocorticoids. *J Biol Chem* **276:** 42714–42721

Wickner S, Maurizi MR, Gottesman S (1999) Posttranslational quality control: folding, refolding, and degrading proteins. *Science* **286:** 1888–1893

Yanagisawa J, Kitagawa H, Yanagida M, Wada O, Ogawa S, Nakagomi M, Oishi H, Yamamoto Y, Nagasawa H, McMahon SB, Cole MD, Tora L, Takahashi N, Kato S (2002) Nuclear receptor function requires a TFTC-type histone acetyl transferase complex. *Mol Cell* **9:** 553–562

Available online at www.sciencedirect.com
SCIENCE DIRECT®
Biochemical and Biophysical Research Communications 322 (2004) 601–608
BBRC
www.elsevier.com/locate/ybbrc

Characterization of BHC80 in BRAF–HDAC complex, involved in neuron-specific gene repression☆

Shigeki Iwase, Aya Januma, Kiyoko Miyamoto, Naomi Shono, Arata Honda, Junn Yanagisawa, Tadashi Baba*

Graduate School of Life and Environmental Sciences and Institute of Applied Biochemistry, University of Tsukuba, Tsukuba Science City, Ibaraki 305-8572, Japan

Received 14 June 2004

Abstract

BRAF–HDAC complex (BHC) has been shown to contain six components, including BHC80, and to mediate REST-dependent transcriptional repression of neuron-specific genes in non-neuronal cells. In this study, we have examined the functional role(s) of BHC80 in mouse tissues and human cultured cells. Two isoforms of mouse BHC80 were predominantly present in the central nervous system and spermatogenic cells. Human cultured cells also contained two isoforms of BHC80. Immunohistochemical analysis showed the presence of mouse BHC80 in the nucleus of neuronal cells in the hippocampus and cerebellum. The C-terminal region of human BHC80 containing PHD zinc-finger domain was capable of binding directly to each of five other components of BHC, and of organizing BHC mediating transcriptional repression. Moreover, two isoforms of human BHC80 were distinguished from each other by reduced binding to HDAC1 and HDAC2, despite the presence of the PHD finger domain. These results suggest that BHC80 presumably serves as a scaffold protein in BHC in neuronal as well as non-neuronal cells. A possible role of BHC80 in spermatogenesis is also suggested.

Keywords: Neuron-specific gene repression; Histone deacetylase; Alternative splicing; Spermatogenesis; Scaffold

A large number of biochemical and genetic evidences have been provided that the changes between active and inactive chromatin states are controlled by multi-protein complexes introduced to DNA [1–4]. In general, transcriptional activators are capable of interacting with histone acetyltransferase (HAT)-containing complexes governing the active chromatin, whereas histone deacetylase (HDAC)-containing complexes recruited by transcriptional repressors convert the chromatin into the inactive state [1]. ATP-dependent chromatin-remodeling complexes also catalyze the active chromatin formation, and promote the access of both HAT and HDAC complexes [2–4]. Although the outline of the well-known nuclear factors involved in the transcriptional machineries is understood, the details still remain to be elucidated.

Many regulatory regions of neuron-specific genes possess negatively acting *cis* elements. For instance, a critical element for the silencing of neuronal genes, repressor element 1/neuron-restrictive silencer element (RE1/NRSE), has been identified in a subset of genes specifically expressed in neuronal cells, including the type II sodium channel, SCG10, and synapsin I genes

☆ This study was partly supported by Grants-in-Aid for Scientific Research on Priority Area, Scientific Research (A), and Exploratory Research from Japan Society for the Promotion of Science (JSPS) and Ministry of Education, Culture, Sports, Science and Technology in Japan (MEXT), and by the 21st Century COE Program from MEXT. S.I. was supported by a Research Fellowship for Young Scientists from JSPS.
* Corresponding author. Fax: +81 29 853 7196.
E-mail address: acroman@sakura.cc.tsukuba.ac.jp (T. Baba).

0006-291X/$ - see front matter © 2004 Elsevier Inc. All rights reserved.
doi:10.1016/j.bbrc.2004.07.163

[5–7]. The RE1/NRSE element is occupied by a zinc finger transcription factor, REST/NRSF [8,9], that regulates the neuronal gene silencing required for normal mouse development [10]. Moreover, REST is capable of recruiting HDAC1, HDAC2, mSin3A, and CoREST [11–14], leading to the inactive chromatin formation and the DNA methylation-dependent silencing of the neuron-specific gene cluster [15].

Recently, BRAF–HDAC complex (BHC) consisting of six subunit proteins, BRAF35, BHC80, BHC110, HDAC1, HDAC2, and CoREST, has been purified from HeLa and HEK293 cells [16]. This protein complex exhibits the histone deacetylation activity, and is recruited to the RE1/NRSE sites of the type II sodium channel and synapsin I genes occupied by REST [16]. Because the recruitment of BHC results in REST-dependent transcriptional repression, BHC is implicated in the regulation of neuron-specific genes presumably through the modulation of chromatin structure. An intriguing finding is that REST-dependent repression is completely abolished by overproduction of BHC80 among the six components of BHC, and the anti-repression activity of BHC80 is partially rescued by addition of BRAF35, HDAC1, or REST [16]. Thus, BHC80 may play a specialized role in BHC. However, little is known of the function of BHC80, despite that this protein has been characterized as a unique protein containing PHD zinc-finger and leucine zipper domains [16].

To elucidate the mechanism of BHC-mediated gene repression, we have focused on BHC80 and examined the molecular basis of mouse and human BHC80, termed mBHC80 and hBHC80, respectively. Two isoforms of BHC80 are produced in mouse tissues and human cultured cells by alternative splicing of the gene transcript. The hBHC80 isoforms are capable of interacting directly with each of five other components in BHC, and are distinguished from each other by reduced binding to HDAC1 and HDAC2. However, both isoforms strongly repress the CMV promoter-derived transcription. These results suggest that BHC80 may function as a scaffold protein in BHC.

Materials and methods

Isolation of cDNA and genomic clones. A 387-bp region at positions 1209–1595 in the cDNA sequence of hBHC80 (GenBank Accession No. AB051483) was amplified by reverse transcriptase (RT)-polymerase chain reaction (PCR) using total cellular RNA from HEK293 cells as a template. The PCR-amplified DNA fragment was labeled with [α-^{32}P]dCTP (3000 Ci/mmol, Amersham–Pharmacia Biotech) by the random-priming procedure [17], and used as a probe to screen recombinant plaques from mouse brain and testis cDNA libraries in λgt10 and λgt11, respectively, as described previously [18].

RT-PCR. Total cellular RNAs were extracted from mouse tissues and human cultured cells, as described [19]. RT-PCR was carried out using a full 3′-RACE kit (Takara Shuzo, Shiga, Japan) according to the manufacturer's protocol. A portion of first-strand cDNA was subjected to PCR using following two sets of oligonucleotide primers: PF1 (5′-AGGATCCGCCTAGTCTAACTGCATCACAG-3′) and PF2 (5′-AGAATTCTGGGCCACAGGCTTGGG-3′); PF3 (5′-AGG ATCCGGTGTACAGTGGGGCTGTCT) and PF4 (5′-GTCACAC ATCAGCAACTGGCCAC-3′).

Antibodies. An N-terminal 93-residue polypeptide of mBHC80 produced in *Escherichia coli* was emulsified with Freund's complete adjuvant (Difco Laboratories), and injected intradermally into female New Zealand White rabbits (SLC, Shizuoka, Japan). The anti-BHC80 antibody was purified by fractionation with ammonium sulfate (0–40% saturation) followed by immunoaffinity chromatography on a column of Sepharose 4B coupled with the above recombinant protein, as described previously [20]. Antibodies against human CoREST and human HDAC2 (H-54) were gifted by Dr. H. Howard [21] and purchased from Santa Cruz Biotechnology (Santa Cruz, CA), respectively.

Preparation of protein extracts. Mouse tissues were homogenized at 0–4 °C in 10 mM Hepes/KOH, pH 7.4, containing 15 mM NaCl, 1 mM EDTA, 0.25 M sucrose, 0.5 mM phenylmethanesulfonyl fluoride, pepstatin A (1 μg/ml), leupeptin (1 μg/ml), and aprotinin (75 U/ml), and centrifuged at 11,000*g* for 10 min at 4 °C. The supernatant solution was used as a source of crude protein extracts. Cytoplasmic and nuclear extracts of mouse tissues were prepared as described [22]. Protein concentration was determined using a Coomassie protein assay reagent kit (Pierce).

Expression plasmids. cDNA clones encoding hBHC80 (KIAA1696) and hBHC110 (KIAA0601) were obtained from Kazusa DNA Research Institute. A CoREST expression vector was gifted by Dr. G. Mandel [14]. cDNA clones encoding HDAC1 and HDAC2 were provided by Dr. A. Fukamizu. Expression plasmids for six isoforms of mBHC80 and hBHC80 were constructed in pcDNA3.1/Myc-His(+)B (Invitrogen). To prepare expression plasmids for GST fusion proteins, cDNA fragments encoding five subunit proteins were introduced into pGEX4T (Amersham–Pharmacia Biotech). GAL4 DNA binding domain was prepared by digestion of pM (Clontech) with restriction enzymes and introduced into the above expression vectors. A luciferase reporter plasmid containing eight UAS upstream of CMV promoter (UAS-CMV-Luc) was constructed using pcDNA3.1 and pGL3-based UAS-TATA-Luc plasmids [23], as described previously [24].

Western blot analysis. Proteins were separated by SDS–polyacrylamide gel electrophoresis (PAGE) and transferred onto Immobilon-P polyvinylidene difluoride membranes (Millipore), as described previously [20]. After blocking with 2% skim milk, the blots were probed by primary antibodies and then incubated with goat anti-rabbit IgG horseradish peroxidase conjugate (Jackson Immunoresearch Laboratories). The immunoreactive proteins were visualized by an ECL Western blotting detection kit (Amersham Pharmacia Biotech).

Immunostaining. Tissues from adult male mice were snap-frozen and embedded in a TissueTek O.C.T compound (Sakura Finetechnical, Tokyo, Japan). Sections (8 μm) were prepared in a Leica CM3000 cryostat, mounted on silanized glass slides, fixed in phosphate-buffered saline (PBS) containing 4% paraformaldehyde, treated with anti-BHC80 antibody, washed, and incubated with horseradish peroxidase-conjugated goat anti-rabbit IgG, as described [20]. The slides were stained with 3,3′-diaminobenzidine as a chromogen, counterstained with 2.5% methyl green, and viewed under an Olympus BX50 microscope. For immunofluorescence microscopy, cells on slides were treated with primary antibody, washed, and incubated with secondary antibody conjugated with Alexa Fluor 488 (Molecular Probes, Eugene, OR), as described [25]. After washing, cells were counterstained with propidium iodide, mounted, and observed under a Leica TCS SP2 confocal laser-scanning microscope.

Immunoprecipitation. Nuclear extracts from HeLa cells were dialyzed against 20 mM Hepes/KOH, pH 7.9, containing 150 mM NaCl, 12.5 mM $MgCl_2$, 0.2 mM EDTA, 0.1% Nonidet P-40, and 1 mM dithiothreitol (binding buffer). Antibodies were incubated at 4 °C for 1 h in PBS (0.2 ml) containing 0.1% Nonidet P-40 and 10 μl of protein A–agarose beads (50% slurry, Pierce). The agarose beads were washed

with the binding buffer to remove unbound antibodies, mixed with nuclear extracts (0.5 mg protein), and then incubated at 4 °C overnight. After centrifugation, the pellet was washed five times with the binding buffer, suspended in a Laemmli buffer, boiled for 5 min, and then subjected to SDS–PAGE.

GST pull-down assays. Recombinant hBHC80 was synthesized in vitro in the presence of ^{35}S-labeled Met (1175 Ci/mmol, Dupont-New England Nuclear) by a TNT T7 Quick Coupled Transcription/Translation system (Promega), as described [26]. DNA fragments encoding GST fusion proteins were expressed in *E. coli* BL21. Cells were lysed by sonicating in PBS containing 10% glycerol, 1 mM dithiothreitol, 0.5 mM phenylmethanesulfonyl fluoride, pepstatin A (1 μg/ml), leupeptin (1 μg/ml), and aprotinin (75 U/ml). After centrifugation at 16,000*g* for 10 min, the supernatant solution was mixed with glutathione–Sepharose gel (Amersham Pharmacia Biotech), incubated at 4 °C for 3 h, and washed five times with the same buffer. The GST fusion protein immobilized on the gel was mixed with ^{35}S-labeled hBHC80 in 50 mM Tris/HCl, pH 7.5, containing 150 mM NaCl, 5 mM EDTA, 0.5% Nonidet P-40, and the above protease inhibitors for 30 min. After the gel was washed five times with the same buffer, proteins on the gel were treated with a Laemmli buffer, and analyzed by SDS–PAGE.

Transient expression and reporter assays. Expression plasmids (1 μg) were introduced into mammalian cells cultured in Dulbecco's modified Eagle's medium (DMEM) supplemented with 10% fetal bovine serum, 100 U/ml penicillin, and 0.1 mg/ml streptomycin at 37 °C under 5% CO_2 in air, using a Fugene transfection reagent (Roche Molecular Biochemicals). After 48-h incubation at 37 °C, cells were harvested by centrifugation, extracted on ice in 20 mM Hepes/KOH, pH7.5, containing 150 mM NaCl, 1 mM EDTA, 1% Triton X-100, 0.5% sodium deoxycholate, 0.1% SDS, and protease inhibitors for 10 min, and re-centrifuged at 16,000*g* for 10 min. Proteins in the supernatant solution were analyzed by Western blot analysis. For luciferase reporter assay, three kinds of plasmids, a reporter plasmid carrying the luciferase gene (45 ng), an hBHC80 effector plasmid (45 ng), and a β-galactosidase expression plasmid (pCMV-β-gal, Clontech) as an internal control (10 ng), were co-transfected into HEK293 cells in 48-well tissue culture dishes. Cells were harvested 48 h after transfection and extracted in a Reporter lysis buffer (Promega). Activities of luciferase and β-galactosidase were measured by a Luciferase assay system kit (Promega) according to the manufacturer's protocol.

Results

Five cDNA clones encoding mBHC80 (GenBank Accession No. AB105178) have been identified from mouse brain and testis cDNA libraries. The cDNA-derived amino acid sequence indicated that mBHC80 shares potential functional domains with hBHC80 (Fig. 1A): an N-terminal Gln (Q)-rich domain, and C-terminal PHD finger and leucine zipper domains present in many transcription factors, including general transcription factors and nuclear receptors [27–29]. Unexpectedly, four out of the five cDNA clones contained different nucleotide sequences in two regions of the open reading frame (5′- and 3′-alternative regions). RT-PCR and subsequent sequence analysis indicated the presence of two (alternative isoform 1, AIF1, and AIF2) and three (AIF3, AIF4, and AIF5) variants in the 5′- and 3′-alternative regions, respectively. AIF1 lacked the 252-nucleotide sequence encoding 84 amino acids in AIF2. AIF4 contained an additional 33-nucleotide sequence in the 3′-alternative region, as compared with AIF3. In AIF5, the 24-nucleotide sequence in AIF3 was replaced by a 165-nucleotide sequence carrying the above 33-nucleotide sequence of AIF4 at the 3′-end. These data suggest the presence of six hypothetical BHC80 isoforms at least in the mouse (BHC80-1 to 6,

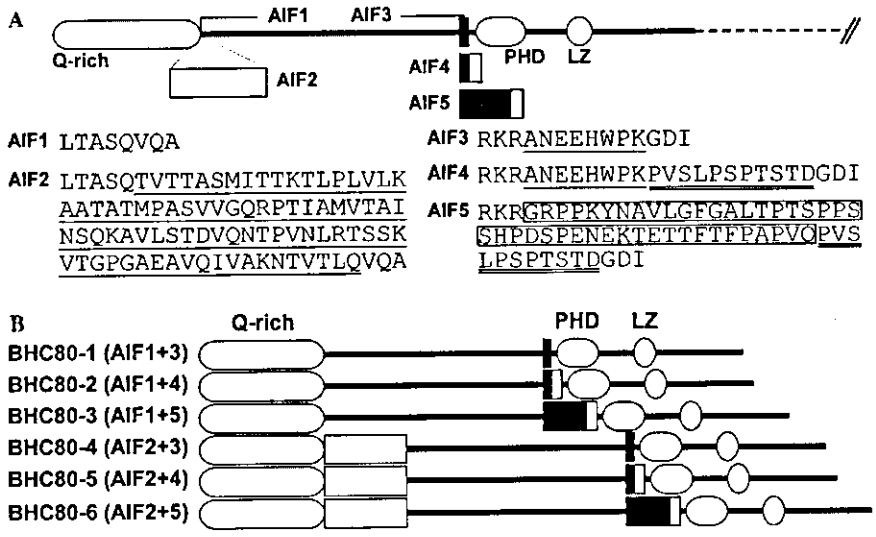

Fig. 1. Six isoforms of BHC80 are possibly produced by alternative splicing. (A) The presence of two (AIF1 and AIF2) and three (AIF3, AIF4, and AIF5) variants in the 5′- and 3′-alternative regions of mouse BHC80, respectively. The variations of the amino acid sequences are shown as follows: open rectangular box, the 84-residue sequence underlined; closed box, the 8-residue sequence underlined; lightly shaded box, the 11-residue sequence double-underlined; darkly shaded box, the 44-residue sequence boxed. PHD and LZ indicate PHD finger and leucine zipper domains, respectively. (B) Schematic representation of six potential isoforms of BHC80.

see Fig. 1B). In human HEK293 and HeLa cells, AIF2, AIF3, and AIF5 were solely amplified by RT-PCR (data not shown), implying that two mRNAs encoding BHC80-4 and BHC80-6 are produced from the hBHC80 gene. It is most likely that 80-kDa BHC80 identified from HeLa cells [16] corresponds to hBHC80-4, because the nucleotide sequences of the amplified AIF2 and AIF3 exactly match with the cDNA sequence of 80-kDa hBHC80.

It has been reported that the hBHC80 gene is expressed in brain in a highly tissue-specific manner [16]. In the present study, Western blot analysis of protein extracts from mouse tissues revealed the abundant presence of 83- and 94-kDa mBHC80 in the brain and testis (Fig. 2A). No immunoreactive protein was apparently detectable in other tissues under the experimental conditions employed. However, a negligibly faint but significant signal for mBHC80 was found in the nuclear extracts from other tissues (data not shown). The 83- and 94-kDa isoforms of mBHC80 were both present in the nuclear extracts of brain and testis, although the cytoplasmic extracts only from the testis contained these two proteins (Fig. 2B). To ascertain the molecular basis of 83- and 94-kDa mBHC80, expression plasmids for six hypothetical mBHC80 isoforms (Fig. 1B) were transfected into mouse NIH3T3 cells, and the recombinant proteins produced were analyzed by Western blotting (Fig. 2C). Endogenous 94-kDa mBHC80 in NIH3T3 cells was slightly detected under the conditions employed. Recombinant mBHC80-5 and mBHC80-6 corresponded to 83- and 94-kDa mBHC80 in mouse tissues, respectively. As shown in Fig. 4D, human HEK293 and HeLa cells possessed 92-kDa hBHC80 as a major isoform, and barely contained an 80-kDa isoform corresponding to hBHC80 previously identified in the BRAF–HDAC complex (BHC) [16]. Recombinant hBHC80-4 and hBHC80-6 were consistent with the 80- and 92-kDa isoforms of hBHC80, respectively. Indeed, when hBHC80-6 fused to a 20-residue peptide tag of FLAG and hemagglutinin (HA) at the N-terminus (FLAG-6) was produced in HEK293 cells, the molecular mass of the recombinant protein was approximately 2 kDa greater than that of recombinant hBHC80-6. These data demonstrate that 83-kDa mBHC80-5, 94-kDa mBHC80-6, and 92-kDa hBHC80-6 are predominantly present in mouse tissues and human cultured cells.

Immunohistochemical analysis using affinity-purified anti-BHC80 antibody indicated that mBHC80 is localized throughout the central nervous system (CNS) in mouse brain, including the cerebellum, hippocampus, and cortex (Figs. 3B–D). Notably, the immunoreactive signals for mBHC80 were found in neuronal cells of granular cell layer and dentate gyrus in cerebellum and

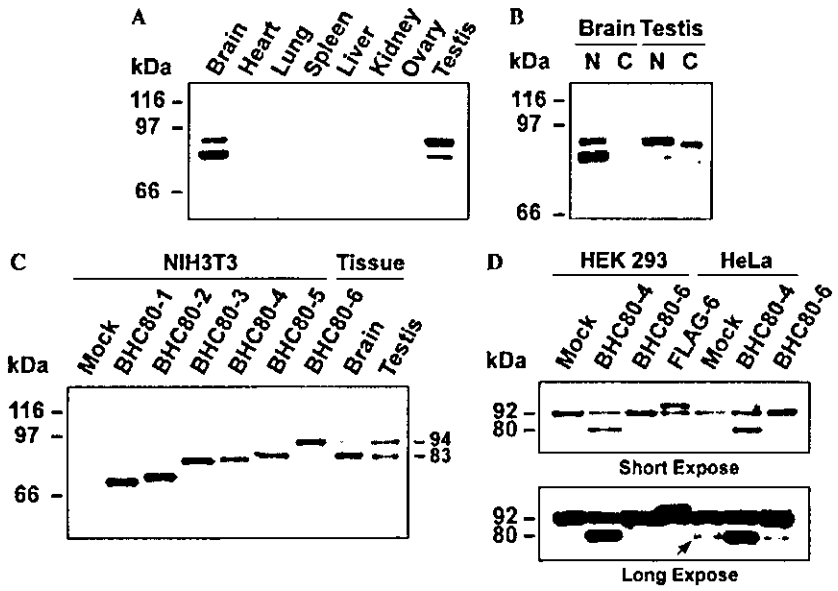

Fig. 2. Tissue distribution and subcellular localization of BHC80. (A) Western blot analysis of protein extracts from eight mouse tissues. Anti-BHC80 antibody recognized 83- and 94-kDa mBHC80 in the brain and testis. (B) Western blot analysis of nuclear (N) and cytoplasmic (C) proteins from mouse brain and testis. (C) Identification of two isoforms of mouse BHC80. Expression plasmids for six hypothetical BHC80 isoforms (Fig. 1B) were transfected into NIH3T3 cells, and the recombinant proteins produced were analyzed by Western blotting. BHC80-5 and BHC80-6 correspond to 83- and 94-kDa BHC80, respectively, in mouse brain and testis. As a control, an expression vector carrying no insert DNA was also transfected (Mock). (D) Identification of two isoforms of human BHC80. Expression plasmids for human BHC80-4, BHC80-6, and FLAG/HA-tagged BHC80-6 (FLAG-6) were transfected into HEK293 and HeLa cells, and the recombinant proteins produced were analyzed by Western blotting. Human cultured cells contain 80- (arrow) and 92-kDa endogenous BHC80, which correspond to recombinant BHC80-4 and BHC80-6, respectively.

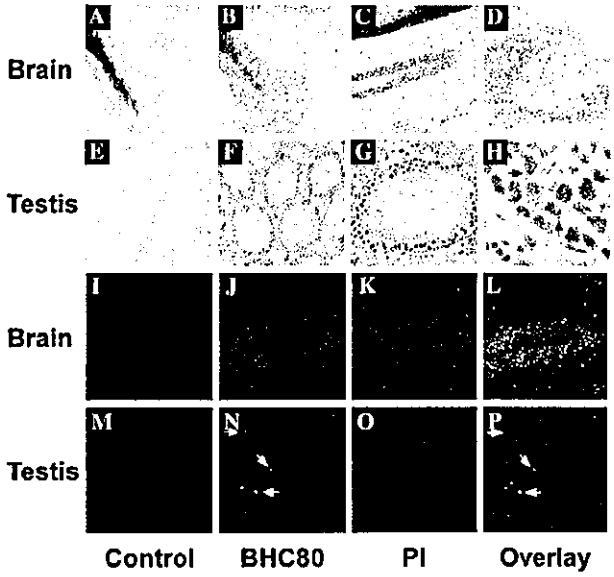

Fig. 3. Location of BHC80 in mouse brain and testis. Sections of mouse brain (A–D) and testis (E–H) were probed by affinity-purified anti-BHC80 antibody and observed under a microscope (magnification, 200×, 400×, and 1000× for A–F, G, and H, respectively). The sections treated only with secondary antibody are represented as negative controls (A,E). The BHC80 signal is found throughout the central nervous system, including the cerebellum (B), hippocampus (C), and cortex (D). In the seminiferous tubules, small dot signals are observed only in spermatocytes (arrows). Indirect immunofluorescence assays (magnification, 400× and 1000× for I–L and M–P, respectively) were also carried out using affinity-purified anti-BHC80 antibody (J,N) and propidium iodide (PI, see K,O). Cells treated only with secondary antibody are represented as negative controls (I,M).

hippocampus, respectively. In the seminiferous tubules, the signals were detected strongly in spermatocytes, and weakly in spermatogonia and round spermatids (panels F–H). Some dot signals were also observed solely in spermatocytes (arrows in panel H). When indirect immunofluorescence assay was carried out, mBHC80 was localized exclusively in the cell nucleus in the entire region of CNS, including the hippocampus (panels J–L). The nuclear localization of mBHC80 was also found in spermatogonia, spermatocytes, and spermatids, although the signals were broad and weak (panels N–P). The dot signals attached only to the nucleus of spermatocytes (panels N and P), as was in the case of a subpopulation of cerebellum cells (data not shown). These data are consistent with the results obtained by Western blot analysis (Fig. 2B).

Despite a very low abundance of 80-kDa hBHC80-4 in HEK293 and HeLa cells (Fig. 2D), this protein has been identified as one of six components in BHC mediating repression of neuron-specific genes through RE1/NRSE regulatory element [16]. To elucidate the functional role of hBHC80-4 in BHC, we examined the direct interaction of recombinant hBHC80-4 with five other subunit proteins fused to GST (Fig. 4A). Two mutant proteins, hBHC80-M1 and hBHC80-M2, lacking the C-terminal 195 and 266 amino acids of hBHC80-4, respectively, were also assessed. hBHC80-4 bound to each of the five subunit proteins, and the binding of hBHC80-4 to BRAF35 and CoREST was stronger than to BHC110, HDAC1, and HDAC2 (Fig. 4B). Although

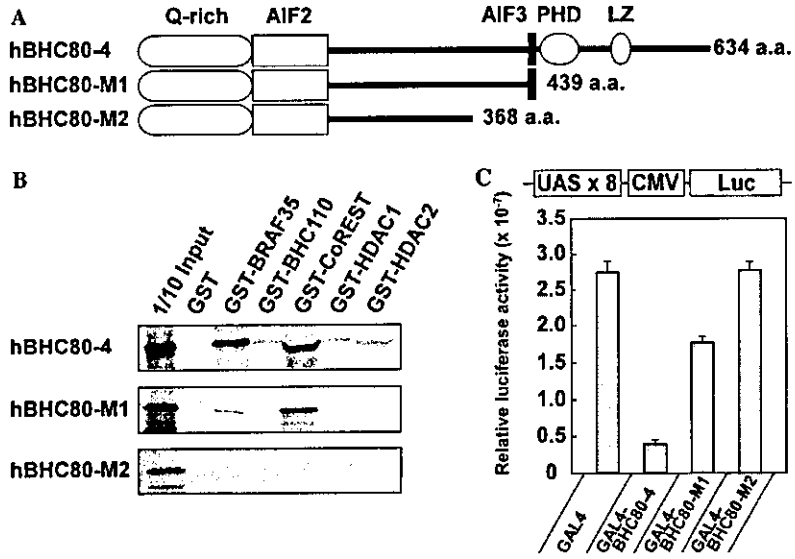

Fig. 4. BHC80 directly interacts with each of five components in BHC and exhibits transcriptional repression activity. (A) Schematic representation of 80-kDa human BHC80 (hBHC80-4) and two mutant proteins (hBHC80-M1 and hBHC80-M2) lacking the C-terminal 195 and 266 amino acids, respectively. PHD and LZ indicate putative PHD finger and leucine zipper domains, respectively. (B) Direct interaction of hBHC80-4 with each of five BHC components fused with GST. GST pull-down assays were carried out using ^{35}S-labeled hBHC80-4, hBHC80-M1, and hBHC80-M2. (C) Transcriptional repression by the C-terminal 195-residue region of hBHC80-4. GAL4-UAS-based luciferase reporter assays were carried out using HEK293 cells. Expression plasmids for hBHC80-4 and two deletion mutants fused to the GAL4 DNA binding domain were co-transfected with a luciferase reporter construct containing eight UAS upstream of CMV promoter (UAS-CMV-Luc). Data are indicated as means ± SD, where $n > 3$.

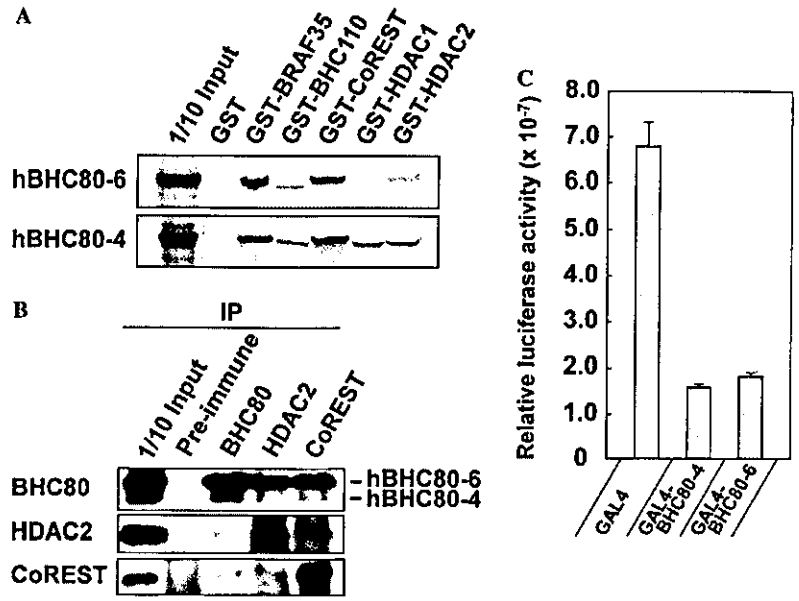

Fig. 5. Functional difference between two isoforms of human BHC80. (A) GST pull-down assays of two BHC80 isoforms. hBHC80-4 and hBHC80-6 corresponding to 80- and 92-kDa human BHC80, respectively, were ^{35}S-labeled and reacted with each of five BHC components fused with GST. (B) Immunoprecipitation analysis of nuclear extracts from HeLa cells. The nuclear extracts were immunoprecipitated (IP) with anti-BHC80, HDAC2, or CoREST antibody, and then subjected to Western blot analysis using anti-BHC80, HDAC2, or CoREST antibody. An IgG fraction of pre-immune serum was used as a control. (C) Transcriptional repression by hBHC80-4 and hBHC80-6. Expression plasmids for hBHC80-4 and hBHC80-6 fused to the GAL4 DNA binding domain were co-transfected into HEK293 cells with a luciferase reporter construct, UAS-CMV-Luc (Fig. 4C). Data are indicated as means ± SD, where $n > 3$.

hBHC80-M1 still bound tightly to CoREST, the binding to BRAF35 and HDAC2 was remarkably reduced. No binding of hBHC80-M1 and hBHC80-M2 to BHC110 and HDAC1, and to all five proteins, respectively, was also found. Thus, hBHC80-4 is capable of interacting directly with each of the five components in BHC. Moreover, the interaction of hBHC80-4 with CoREST requires the 71-residue region at positions 369–439 in hBHC80-4, whereas the C-terminal 195-residue region containing the PHD finger domain may play an important role in the binding of hBHC80-4 to BRAF35, BHC110, HDAC1, or HDAC2.

To examine whether hBHC80-4 affects gene transcription, GAL4-UAS-based luciferase reporter assays were carried out using HEK293 cells (Fig. 4C). Expression plasmids for hBHC80-4, hBHC80-M1, and hBHC80-M2 fused to the GAL4 DNA binding domain were co-introduced into cells with a reporter plasmid carrying eight GAL4 binding sites upstream of the CMV promoter. The CMV promoter-derived transcription was 86% and 36% reduced by expression of GAL4-hBHC80-4 and GAL4-hBHC80-M1, respectively, whereas GAL4-hBHC80-M2 exhibited no repression activity. These data demonstrate the essential role of the C-terminal 195-residue region of hBHC80-4 in the transcriptional repression.

We next examined whether hBHC80-6 is functionally distinguishable from hBHC80-4. GST pull-down assays indicated that the interaction of hBHC80-6 with HDAC1 or HDAC2 is noticeably weak, as compared with hBHC80-4 (Fig. 5A). However, immunoprecipitation analysis of nuclear extracts from HeLa cells using antibodies against BHC80, HDAC2, and CoREST indicated that hBHC80-6 as well as hBHC80-4 is co-localized with HDAC2 and CoREST probably in BHC (Fig. 5B). In addition, both hBHC80-4 and hBHC80-6 strongly repressed the CMV promoter-derived transcription (Fig. 5C). Thus, the functions of these two hBHC80 isoforms are essentially similar to each other, except the binding to HDAC1 and HDAC2.

Discussion

This study describes a possible functional role of BHC80 as a component of BRAF–HDAC complex (BHC) mediating REST-dependent transcriptional repression of neuron-specific genes in non-neuronal cells. Both 83- and 94-kDa mBHC80 are predominantly present in CNS and germ cells of the brain and testis (Figs. 2 and 3). Immunohistochemical analysis clearly demonstrates the presence of mBHC80 in the nucleus of neurons of hippocampus and cerebellum (Fig. 3). Because REST is also localized in neuronal cells [30–32] as well as in non-neuronal cells and undifferentiated neuronal progenitors [8,9], our data suggest that REST and